

Kernel-Based Distributed Q-Learning: A Scalable Reinforcement Learning Approach for Dynamic Treatment Regimes

Di Wang, Yao Wang, Shao-Bo Lin ^{*}

Center for Intelligent Decision-Making and Machine Learning, School of Management, Xi'an Jiaotong University, Xi'an, China

In recent years, large amounts of electronic health records (EHRs) concerning chronic diseases have been collected to facilitate medical diagnosis. Modeling the dynamic properties of EHRs related to chronic diseases can be efficiently done using dynamic treatment regimes (DTRs). While reinforcement learning (RL) is a widely used method for creating DTRs, there is ongoing research in developing RL algorithms that can effectively handle large amounts of data. In this paper, we present a scalable kernel-based distributed Q-learning algorithm for generating DTRs. We perform both theoretical assessments and numerical analysis for the proposed approach. The results demonstrate that our algorithm significantly reduces the computational complexity associated with the state-of-the-art deep reinforcement learning methods, while maintaining comparable generalization performance in terms of accumulated rewards across stages, such as survival time or cumulative survival probability.

Key words: Q-learning, dynamic treatment regimes, distributed learning, kernel ridge regression

1. Introduction

Patients with chronic diseases, such as cancer, diabetes, and mental disease, usually undergo a period of initial treatment, disease recurrence, and salvage treatment. Explicitly specifying the relationship of treatment type and drug dosage with patient response is generally difficult, so practitioners have to use protocols in which each patient receives a similar treatment based on the average responses of previous patients with similar cases. However, illnesses respond heterogeneously to treatment. For example, a study on schizophrenia (Ishigooka et al. 2000) discovered that patients

^{*} Corresponding authors: sblin1983@gmail.com

using the exact same antipsychotic experience drastically varied outcomes; some patients experience few adverse events with improved clinical outcomes, whereas others have to discontinue treatment due to worsening symptoms. This has motivated researchers to advocate dynamic treatment regimes (DTRs) to determine treatments dynamically and individually based on clinical observations of patients (Murphy 2005a, Chakraborty and Moodie 2013, Almirall and Chronis-Tuscano 2016).

A DTR is defined by a set of sequential decision rules; each rule takes the clinical observations of a patient at certain key points as input and returns the treatment action of doctors as output (Tsiatis et al. 2019). In this way, the design of a DTR can be considered a sequential decision-making problem and suits the reinforcement learning (RL) framework (Sutton and Barto 2018), in which states, actions, rewards, and policies correspond to the clinical observations of patients, treatment options, treatment outcomes, and series of decision rules, respectively. RL simultaneously addresses sequential decision-making problems with sampled, evaluative, and delayed feedback, which naturally makes it a desirable tool for developing ideal DTRs.

Q-learning (Watkins and Dayan 1992) is a typical temporal-difference algorithm that produces a sequence of high-quality actions in RL and has been substantially developed in the past decades in health care (Oh et al. 2022). Different from other applications, Q-learning for DTRs with a finite horizon (typically small and not exceeding a few tens) commonly has the following important characteristics:

- Data structure: When a patient's chronic disease is not effectively treated or managed through a particular treatment plan, they may seek alternative treatment options from other doctors, resulting in treatment records with limited duration. Additionally, in Q-learning for DTRs, doctors typically have a limited number of treatment options to choose from based on patients' treatment histories (Tsiatis et al. 2019, Chap.1.4). However, for a given treatment decision, the clinical observations of patients can be unpredictable, resulting in an infinite number of states. This makes Q-learning for DTRs distinct from classical tabular-based Q-learning, which focuses on finite actions and states (Gosavi 2009). To summarize, DTRs have finite horizons, and each stage of Q-learning for DTRs has a finite number of actions but an infinite number of states.

• Task orientation: For DTRs with a small number of stages, like non-small-cell lung cancer (NSCLC) patients typically undergoing one to three treatment lines (Socinski and Stinchcombe 2007), treatment decisions at each critical point in Q-learning are crucial for determining patient outcomes, regardless of timing. Hence, assuming one treatment phase is more critical than others is inappropriate, and the standard Q-learning reward discounting method is unsuitable for such DTRs.

• Quality guarantee: Quality is crucial in medical treatment, as even a small mistake may result in extremely negative outcomes for patients. This necessitates not only a strong understanding of treatment decisions but also solid theoretical guarantees supporting the effectiveness. This requirement eliminates the use of some heuristic yet intricate designs of Q-learning (Oroojlooyjadid et al. 2022) for generating DTRs.

• Computational costs: This increase in data size poses significant scalability challenges for the Q-learning algorithms, in terms of storage and computational complexity. This scalability requirement excludes the popular deep learning in DTR since it inherently entails a substantial number of parameters and hyperparameter, markedly escalating the computational resource requirements.

The characteristics discussed above place strict limitations on the use of Q-learning for generating DTRs. The need for quality guarantees excludes the commonly used linear Q-learning (Murphy 2005b), and the demands for computational efficiency and interpretability make the widely adopted deep Q-learning (Oroojlooyjadid et al. 2022) unsuitable for DTRs. In this paper, we aim to create a scalable Q-learning algorithm that has solid theoretical guarantees for DTRs.

1.1. Mathematical formulation of Q-learning for DTRs

DTRs often involve T -stage treatment decision problems. Let $s_t \in \mathcal{S}_t$ be the pretreatment information (or status) and $a_t \in \mathcal{A}_t$ be the treatment decision (or action) at stage t , where \mathcal{S}_t and \mathcal{A}_t are sets of pretreatment information and treatment decisions, respectively. A history of personalized treatment is generated in the form of $\mathcal{T}_T = \{s_{1:T+1}, a_{1:T}\}$, where s_{T+1} is the status after all treatment decisions, $s_{1:t}$ and $a_{1:t}$ denote all historical status and actions recorded from stage 1 to stage t ,

i.e., $s_{1:t} = \{s_1, s_2, \dots, s_t\}$, $a_{1:t} = \{a_1, a_2, \dots, a_t\}$. Similarly, $\mathcal{S}_{1:t}$ and $\mathcal{A}_{1:t}$ represent the status space and action space, respectively, formed from stage 1 to stage t , i.e., $\mathcal{S}_{1:t} = \mathcal{S}_1 \times \mathcal{S}_2 \times \dots \times \mathcal{S}_t$ and $\mathcal{A}_{1:t} = \mathcal{A}_1 \times \mathcal{A}_2 \times \dots \times \mathcal{A}_t$. Let $R_t : (\mathcal{S}_{1:t+1}, \mathcal{A}_{1:t}) \rightarrow \mathbb{R}$ be the clinical outcome following the decision a_t , which depends on the pretreatment information $s_{1:t+1}$ and treatment history $a_{1:t}$. In cancer treatment, for example, R_t can be set as the tumor size or the survival time when the t -th treatment decision is made. Throughout the paper, we use capital letters (A_1, A_2 , etc.) to denote random variables and lowercase letters (a_1, a_2 , etc.) to represent their realization.

A DTR $\pi = (\pi_1, \dots, \pi_T)$, where $\pi_t : \mathcal{S}_{1:t} \times \mathcal{A}_{1:t-1} \rightarrow \mathcal{A}_t$, is a set of rules for personalized treatment decisions at all T stages. The optimal DTR is that which maximizes the overall outcome of interest $\sum_{t=1}^T R_t(s_{1:t+1}, a_{1:t})$ in terms of designing suitable treatment rules $\pi = (\pi_1, \dots, \pi_T)$. Our analysis is cast in a random setting to quantify the overall outcome (Murphy 2005b). Denote by $\rho_t(s_t | s_{1:t-1}, a_{1:t-1})$ the transition probability of s_t conditioned on $s_{1:t-1}$ and $a_{1:t-1}$. The value of a DTR π at stage t is defined by

$$V_{\pi,t}(s_{1:t}, a_{1:t-1}) = E_{\pi} \left[\sum_{j=t}^T R_j(S_{1:j+1}, A_{1:j}) \mid S_{1:t} = s_{1:t}, A_{1:t-1} = a_{1:t-1} \right],$$

where E_{π} is the expectation with respect to the distribution

$$P_{\pi} = \rho_1(s_1) \mathbf{1}_{a_1=\pi_1(s_1)} \prod_{t=2}^T \rho_t(s_t | s_{1:t-1}, a_{1:t-1}) \mathbf{1}_{a_t=\pi(s_{1:t}, a_{1:t-1})} \rho_{T+1}(s_{T+1} | s_{1:T}, a_{1:T}),$$

and $\mathbf{1}_W$ is the indicator of the event W . Denote the optimal value function of π at stage t as

$$V_t^*(s_{1:t}, a_{1:t-1}) = \max_{\pi \in \Pi} V_{\pi,t}(s_{1:t}, a_{1:t-1}),$$

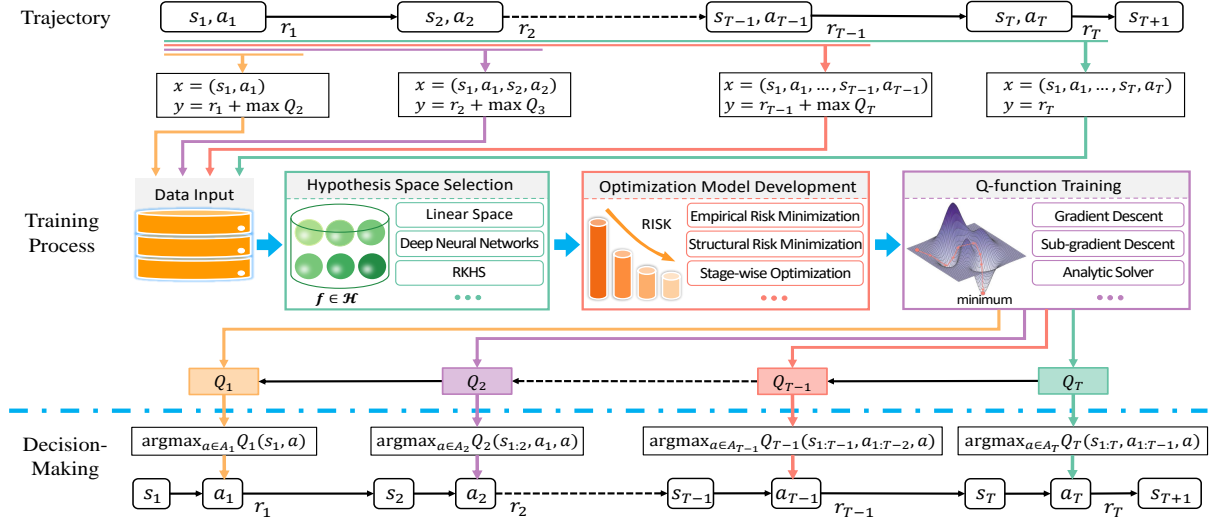
where Π is the collection of all treatments. We aim to find a policy $\hat{\pi}$ to minimize $V_1^*(s_1) - V_{\hat{\pi},1}(s_1)$.

Let $p_t(a_t | s_{1:t}, a_{1:t-1})$ be the probability that a decision a_t is made given the history $\{s_{1:t}, a_{1:t-1}\}$. Define the optimal time-dependent Q -function by

$$Q_t^*(s_{1:t}, a_{1:t}) = E[R_t(S_{1:t+1}, A_{1:t}) + V_{t+1}^*(S_{1:t+1}, A_{1:t}) | S_{1:t} = s_{1:t}, A_{1:t} = a_{1:t}], \quad (1)$$

where E is the expectation with respect to the distribution $P := P_{T+1}$ and

$$P_t = \rho_1(s_1) p_1(a_1 | s_1) \prod_{j=2}^t \rho_j(s_j | s_{1:j-1}, a_{1:j-1}) p_j(a_j | s_{1:j}, a_{1:j-1}). \quad (2)$$

Figure 1 Training and decision-making flows of Q-learning.

Given the definition of V_t^* , it is easy to derive Murphy (2005b)

$$V_t^*(s_{1:t}, a_{1:t-1}) = V_{\pi^*, t}(s_{1:t}, a_{1:t-1}) = E_{\pi^*} \left[\sum_{j=t}^T R_j(S_{1:j+1}, A_{1:j}) \mid S_{1:t} = s_{1:t}, A_{1:t-1} = a_{1:t-1} \right],$$

where π^* is the optimal policy and consequently

$$V_t^*(s_{1:t}, a_{1:t-1}) = \max_{a_t} Q_t^*(s_{1:t}, a_{1:t}), \quad (3)$$

showing that the optimal treatment decisions can be determined by maximizing the optimal Q -functions. Thus, researchers have developed efficient algorithms for finding optimal Q -functions in the realm of RL (Murphy 2005b). With $Q_{T+1}^* = 0$, the definition of Q_t^* indicates that

$$Q_t^*(s_{1:t}, a_{1:t}) = E \left[R_t(S_{1:t+1}, A_{1:t}) + \max_{a_{t+1}} Q_{t+1}^*(S_{1:t+1}, A_{1:t}, a_{t+1}) \mid S_{1:t} = s_{1:t}, A_{1:t} = a_{1:t} \right] \quad (4)$$

for $t = T, T-1, \dots, 1$. This property connects Q -functions with the well-known regression function (Györfi et al. 2006) in supervised learning as follows. Define $\mathcal{X}_t = \mathcal{S}_{1:t} \times \mathcal{A}_{1:t}$, and denote \mathcal{L}_t^2 as the space of square-integrable functions defined on \mathcal{X}_t with respect to P_t .

Write

$$x_t := \{s_{1:t}, a_{1:t}\} \in \mathcal{X}_t, \quad \text{and} \quad y_t^* := R_t(s_{1:t+1}, a_{1:t}) + \max_{a_{t+1}} Q_{t+1}^*(s_{1:t+1}, a_{1:t}, a_{t+1}). \quad (5)$$

Q_t^* can be regarded as the regression function of data (x_t, y_t^*) and written as

$$Q_t^* = E[Y_t^*|X_t], \quad t = T, T-1, \dots, 1. \quad (6)$$

Therefore, the standard approach in statistical learning theory (Györfi et al. 2006) yields

$$Q_t^* = \arg \min_{Q_t \in \mathcal{L}_t^2} E \left[(Y_t^* - Q_t(X_t))^2 \right], \quad t = T, T-1, \dots, 1, \quad (7)$$

showing that optimal Q -functions can be obtained by solving T least squares problems. As shown in Figure 1, through the iterative generation of input–output pairs, Q-learning can be regarded as a series of supervised learning problems and incorporates four steps: hypothesis space selection, optimization model development, Q -function training, and policy search. The hypothesis space selection step focuses on selecting a class of functions that encodes some a priori information and determines the formats of Q -functions. The optimization model development step involves mathematically defining the Q -functions via a sequence of optimization problems. After the optimization model is developed, a feasible optimization algorithm should be designed in the Q -function training step to derive Q -functions. Finally, the policy search step searches for the best possible policies for choosing appropriate actions by maximizing the Q -functions.

1.2. Problem setting

We are interested in Q-learning with T stages whose state space \mathcal{S}_t is an infinite continuous space and whose action space \mathcal{A}_t is a discrete set of finite elements. To suit different chronic diseases, the proposed Q-learning algorithm for DTRs should be feasible, efficient, and theoretically sound for a large number of reward functions because different reward functions usually correspond to various chronic diseases (Padmanabhan et al. 2017). The setting of Q-learning in this paper is shown in Table 1.

As the starting point of Q-learning, hypothesis spaces regulate the format and properties of the Q -functions to be learned and determine the type of optimization models to be developed. Linear spaces (Murphy 2005b) and deep neural networks (François-Lavet et al. 2018) are widely known hypothesis spaces for Q-learning. However, linear spaces have limited expressive power and

Table 1 Setting of Q-learning for DTRs.

Horizon	Action space	State space	Reward function	Discount	Quality
T	Finite	Continuous	Smooth	No	Generalization error

cannot adapt to different reward functions, frequently performing poorly for chronic diseases, such as cancer and sepsis (Yu et al. 2021, Sec.4), whereas deep neural networks lack solid theoretical guarantees and are usually time consuming. Since Q-learning for DTRs requires a perfect balance between an expressive hypothesis space for quality guarantees and a simple hypothesis space for scalability, we are faced with the following challenge:

PROBLEM 1. How can a hypothesis space be designed to equip Q-learning for DTRs to avoid the limitations of both linear spaces and deep neural networks simultaneously?

Once the hypothesis space is determined, optimization models are crucial in defining Q-functions. In general, a good optimization model for Q-learning for DTRs should be solvable, scalable, and interpretable. Solvability means that the developed model can be solved using standard optimization algorithms like gradient descent. Scalability implies that the cost of solving the optimization problem is reasonable. Interpretability means that the developed model is easy to understand. Optimization models with good solvability, scalability, and interpretability can be easily developed for linear hypothesis spaces, but for nonlinear spaces, these properties are difficult to achieve. Therefore, we focus on the following problem:

PROBLEM 2. How to develop solvable, scalable, and interpretable optimization models for Q-learning for DTRs to optimize the performance of chosen nonlinear or infinite hypothesis spaces?

The solutions to Problems 1 and 2 are sufficient to develop DTRs through Q-learning. With the emphasis on the quality guarantee of Q-learning for DTRs, we ultimately focus on the following problem:

PROBLEM 3. How can the quality of the resulting DTRs be theoretically measured and how can solid theoretical guarantees be provided for it?

Unlike other applications, such as recommendations and supply chain management, which use regret (Liu and Su 2022) to measure the quality of the developed policies, DTRs focus on the final treatment outcomes, regardless of the median treatment processes, to fully explore the values of the initial states. This means that new analysis tools are required for theoretical guarantees.

1.3. Our contributions

We develop a scalable Q-learning algorithm based on kernel ridge regression (KRR) (Caponnetto and De Vito 2007) for DTRs to address the above problems. Our main contributions are as follows:

- Methodological novelty: Breaking down Q-learning into T least squares regression problems, we combine distributed learning (Zhang et al. 2015) and KRR to estimate Q-functions. Specifically, we adopt distributed regularized least squares over specific RKHS as the optimization model in Q-learning. This approach avoids the quality limitations of linear Q-learning and addresses the computational efficiency issues of deep Q-learning, simultaneously.
- Theoretical Novelty: We propose a novel integral operator approach to analyze the generalization error of Q-learning. Our theoretical results indicate that distributed learning does not increase the generalization error, provided the data are not divided into too many subsets. Additionally, the generalization error bounds we derived are independent of the input dimensions, indicating that the proposed algorithm scales well with respect to the dimensionality of the problem.
- Numerical Novelty: We evaluate the proposed algorithm against linear Q-learning and several state-of-the-art deep RL methods in two types of clinical trials for cancer treatments. Our numerical results show that the performance of our approach is consistently better than that of linear Q-learning and comparable to that of deep RL methods. In terms of computational costs, our approach requires significantly less training time than deep RL methods. These results demonstrate the effectiveness and efficiency of the proposed kernel-based distributed Q-learning for DTRs.

The rest of this paper is organized as follows. Section 2 introduces some related work and compares our approach with theirs. In Section 3, we explain the proposed kernel-based distributed Q-learning algorithm for DTRs. In Section 4, we study the theoretical behaviors of the proposed

algorithm by establishing two generalization error bounds, whose proofs are given in the appendix. In Section 5, two simulations are conducted to illustrate how the proposed algorithm outperforms linear Q-learning and deep RL methods.

2. Related Work and Comparisons

EHRs have been widely used in health care decisions regarding chronic diseases over the last decade. Q-learning is a promising approach to utilizing EHRs to yield high-quality DTRs and has gained fruitful clinical effects in improving the quality of health care decisions (Tsiatis et al. 2019, Yu et al. 2021). In particular, Zhao et al. (2009) used support vector regression (SVR) and extremely randomized trees to fit approximated Q-functions for agent dosage decision-making in chemotherapy; Humphrey (2017) employed classification and regression trees (CART), random forests, and a modified version of multivariate adaptive regression splines to estimate Q-values for an advanced generic cancer trial; Tseng et al. (2017) presented a multicomponent deep RL framework for patients with NSCLC in which a deep Q-network (DQN) maps states into potential dose schemes to optimize future radiotherapy outcomes; Raghu et al. (2017) proposed a fully connected dueling double DQN approach to learn an approximation of the optimal action–value function for sepsis treatment. The reader is referred to Tables III and IV of (Yu et al. 2021) for more related work on Q-learning for DTRs.

Compared with these methods, our approach possesses three main novelties. First, we employ kernel-based Q-learning to generate DTRs because the design of kernel methods satisfies the high requirements of Q-learning for DTRs (the hypothesis space of a kernel method is large enough, and the derived estimator is in a linear space). Second, we focus on distributed Q-learning algorithms for DTRs that scale well according to the data size. Such a scalable variant of Q-learning for DTRs has not been considered in the literature. Finally, we provide solid theoretical guarantees for the proposed Q-learning approach in the framework of statistical learning theory (Murphy 2005b), which is beyond the scope of the above mentioned papers.

Note that there are also asynchronous parallel deep Q-learning algorithms, such as the distributed method proposed by Ong et al. (2015), which can accelerate computations through distributed

asynchronous gradient calculations. However, our method differs significantly. Specifically, their Q-function remains consistent across different stages, whereas ours is stage-dependent. Regarding communication, their methods entail costs per parameter iteration, while ours involves only one communication per stage. More importantly, their distributed nodes require a real environment to collect experiences, but ours trains solely on historical data without a real environment model.

We then introduce several theoretical results of Q-learning. From the theoretical analysis viewpoint, the quality of Q-learning has been extensively studied, and can be roughly classified into two types (Levine et al. 2020, Figueiredo Prudencio et al. 2024). The one is for online Q-learning, which constantly interacts with the environment to collect new experiences with the latest policy before updating the Q-function. In particular, Kearns and Singh (1998) proposed a framework to deduce the finite-time convergence rates (i.e., sample size bounds) for Q-learning algorithms; Even-Dar and Mansour (2003) derived a sufficient condition of the learning rate in gradient-based linear Q-learning to guarantee the convergence (stability) of Q-learning; Xu et al. (2007) proposed a kernel-based least squares policy iteration algorithm and presented the convergence analysis; Wainwright (2019) developed a variance reduction technique to improve the performance of Q-learning and proved that it achieves the minimax optimal sample complexity up to a logarithmic factor in the discount complexity; Liu and Su (2022) studied regret bounds for kernel-based Q-learning. The other is for offline Q-learning (fitted-Q-iteration, FQI), which learns Q-functions from a static data set of transitions and no longer interacts with the environment. Specifically, Murphy (2005b), Goldberg and Kosorok (2012), Wang et al. (2020), and Oh et al. (2022) studied the generalization error of linear Q-learning; Fan et al. (2020) deduced a generalization error estimate for deep Q-learning; Duan et al. (2021) provided upper bounds on the generalization performance of Q-learning by using Rademacher complexity. However, the setting of Q-learning studied in the current paper is different from most of these works, as we are concerned with the states, actions, and rewards in Table 1. For example, except for (Murphy 2005b, Goldberg and Kosorok 2012, Oh et al. 2022), all the above studies focused on Q-learning with large (or even infinite) horizons and discounted rewards.

The most closely related works to ours are (Oh et al. 2022) and (Liu and Su 2022). The former deduced a similar generalization error to ours for linear Q-learning under the same setting as in the present paper, whereas the latter aimed to derive regret bounds for kernel-based Q-learning. The differences between our work and (Oh et al. 2022) are as follows. We study kernel-based distributed Q-learning rather than linear Q-learning. The main advantage of utilizing an RKHS as the hypothesis space is the excellent expressive power over linear spaces. Moreover, we employ a novel integral operator approach to deduce the generalization error of Q-learning for DTRs rather than using the standard covering number approach. The generalization error bounds in our paper, derived under weaker assumptions on data distribution, are considerably tighter than the results in (Oh et al. 2022). The main differences between our work and (Liu and Su 2022) are three aspects. First, we are interested in generalization error analysis, whereas Liu and Su (2022) focused on regret analysis. Because the goal of treatment is to find a DTR $\hat{\pi}$ that minimizes $V_1^*(s_1) - V_{\hat{\pi},1}(s_1)$, the generalization error $E[V_1^*(s_1) - V_{\hat{\pi},1}(s_1)]$ is more appropriate for DTRs than the regret $\sum_{t=1}^T ((V_t^*(s_{1:t}, a_{1:t-1}) - V_{\hat{\pi},t}(s_{1:t}, a_{1:t-1}))$. Furthermore, Liu and Su (2022) imposed strong restrictions on the kernel (linear kernel or Gaussian kernel), whereas our approach is available to any positive-definite kernel. Finally, as we use a distributed version of kernel methods, the computational costs of the proposed approach for DTRs are much less than those of the kernel-based algorithms in (Liu and Su 2022).

3. Kernel-Based Distributed Q-Learning for DTRs

Since (7) is defined by expectation, Q_t^* cannot be derived directly. The only thing we have access to is a set of records of personalized treatments $D := \{\mathcal{T}_{i,T}, r_{i,1:T}\}_{i=1}^{|D|}$, where samples in $\{\mathcal{T}_{i,T}\}_{i=1}^{|D|} = \{(s_{i,1:T+1}, a_{i,1:T})\}_{i=1}^{|D|}$ are assumed to be drawn independently and identically according to P , $r_{i,t} := R_t(s_{i,1:t+1}, a_{i,1:t})$, and $|D|$ denotes the cardinality of the set D . We derive an approximation of Q_t^* using D , which is a standard regression problem in supervised learning. Empirically, by setting $\hat{Q}_{T+1} = 0$, we can compute Q-functions by solving T structural risk minimization problems

$$\hat{Q}_t(s_{1:t}, a_{1:t}) = \arg \min_{Q_t \in \mathcal{H}_t} \mathbb{E}_D \left[\left(R_t(S_{1:t+1}, A_{1:t}) + \max_{a_{t+1}} \hat{Q}_{t+1}(S_{1:t+1}, A_{1:t}, a_{t+1}) - Q_t(S_{1:t}, A_{1:t}) \right)^2 \right] + \lambda \Omega(Q_t) \quad (8)$$

for $t = T, T-1, \dots, 1$, where \mathbb{E}_D is the empirical expectation, \mathcal{H}_t is a parameterized hypothesis space, $\Omega(Q_t)$ is some structures of Q_t , and λ is a tunable parameter to balance the empirical risk and structure. Our goal is to find a suitable \mathcal{H}_t and $\Omega(Q_t)$ so that \hat{Q}_t is close to Q_t^* .

Before presenting the detailed algorithm, we elucidate the reasons for using kernel-based Q-learning:

- Q-learning for DTRs can be regarded as a T -stage least squares regression problem, and kernel methods are well-developed learning schemes that exhibit optimal generalization performance (Caponnetto and De Vito 2007, Lin et al. 2017) in least squares regression, which implies that kernel methods perform excellently with strong theoretical guarantees in each stage.
- Numerous scalable variants of kernel methods (Zhang et al. 2015, Rudi et al. 2015, Meister and Steinwart 2016) have been proposed and successfully used. These variants provide guidance for the development of scalable Q-learning algorithms for DTRs.
- Linear hypothesis spaces are beneficial for computations but have poor generalization performance. Conversely, the complex structures of deep neural networks enable deep Q-learning in generalization but are frequently time consuming. Kernel methods balance Q-learning with linear spaces and deep Q-learning in terms that kernelized Q-learning outperforms linear Q-learning in generalization and has a smaller computational burden than deep Q-learning.

Based on these, we use KRR (Caponnetto and De Vito 2007, Zhang et al. 2015) to derive an approximation of Q_t^* empirically based on the given dataset D . Let $K(x, x') := K_t(x, x')$ be a Mercer kernel, where $x, x' \in \mathcal{X}_t$, and $\mathcal{H}_{K,t}$ be the corresponding RKHS endowed with the norm $\|\cdot\|_{K,t}$. Given regularization parameters λ_t for $t = 1, \dots, T$, if we set $Q_{D,\lambda_{T+1},T+1} = 0$ with $\lambda_{T+1} = 0$, then the Q -functions can be empirically defined by

$$Q_{D,\lambda_t,t} = \arg \min_{Q_t \in \mathcal{H}_{K,t}} \frac{1}{|D|} \sum_{i=1}^{|D|} (y_{i,t} - Q_t(s_{i,1:t}, a_{i,1:t}))^2 + \lambda_t \|Q_t\|_{K,t}^2, \quad t = T, T-1, \dots, 1, \quad (9)$$

where

$$y_{i,t} := r_{i,t} + \max_{a_{t+1} \in \mathcal{A}_{t+1}} Q_{D,\lambda_{t+1},t+1}(s_{i,1:t+1}, a_{i,1:t}, a_{t+1}). \quad (10)$$

Through straightforward computations, $Q_{D,\lambda_t,t}$ can be explicitly formulated as

$$Q_{D,\lambda_t,t} = \sum_{i=1}^{|D|} \alpha_{i,t} \cdot K((s_{i,1:t}, a_{i,1:t}), \cdot) \quad (11)$$

Here, $\boldsymbol{\alpha}_t := [\alpha_{1,t}, \dots, \alpha_{|D|,t}]^\top = (\mathbb{K}_t + \lambda_t |D| \mathbb{I})^{-1} \mathbf{y}_t$ and $K((s_{i,1:t}, a_{i,1:t}), \cdot)$ represents the kernel function evaluated at the point $(s_{i,1:t}, a_{i,1:t})$, where $\mathbf{y}_t := [y_{1,t}, \dots, y_{|D|,t}]^\top$ and \mathbb{K}_t denotes the kernel matrix whose (i, j) -th element is $K((s_{i,1:t}, a_{i,1:t}), (s_{j,1:t}, a_{j,1:t}))$. In this way, (9) can be solved backward to derive a sequence of estimators $\{Q_{D,\lambda_t,t}\}_{t=1}^T$. We then define the corresponding KRR for DTRs (KRR-DTR) by $\pi_{D,\vec{\lambda}} = (\pi_{D,\lambda_1,1}, \dots, \pi_{D,\lambda_T,T})$ with

$$\pi_{D,\lambda_t,t}(s_{1:t}, a_{1:t-1}) = \arg \max_{a_t \in \mathcal{A}_t} Q_{D,\lambda_t,t}(s_{1:t}, a_{1:t-1}, a_t), \quad t = 1, \dots, T. \quad (12)$$

Solving KRR (9) requires $\mathcal{O}(|D|^3)$ floating computations in each stage, which makes KRR time consuming for large-scale datasets. A scalable variant of (9) should be developed to reduce the computational burden so that (9) can be successfully utilized to handle large-scale datasets to generate a DTR of high-quality. Distributed learning equipped with a divide-and-conquer strategy (Zhang et al. 2015, Lin et al. 2017, 2020) is preferable for this purpose. Kernel-based distributed Q-learning can be divided into four steps: division, local processing, synthesis, and iteration.

- *Division*: Randomly divide the dataset D into m disjoint subsets D_j according to the uniform distribution, that is, $D = \bigcup_{j=1}^m D_j$, $D_j \cap D_{j'} = \emptyset$ for $j \neq j'$. Denote $D_j = \{s_{i,j,1:T+1}, a_{i,j,1:T}, r_{i,j,1:T}\}_{i=1}^{|D_j|}$.
- *Local Processing*: Initialize $\bar{Q}_{D,\lambda_{T+1},T+1} \equiv 0$, where $\lambda_{T+1} = 0$. At the t -th stage, calculate the output of the i -th sample in the j -th data subset as

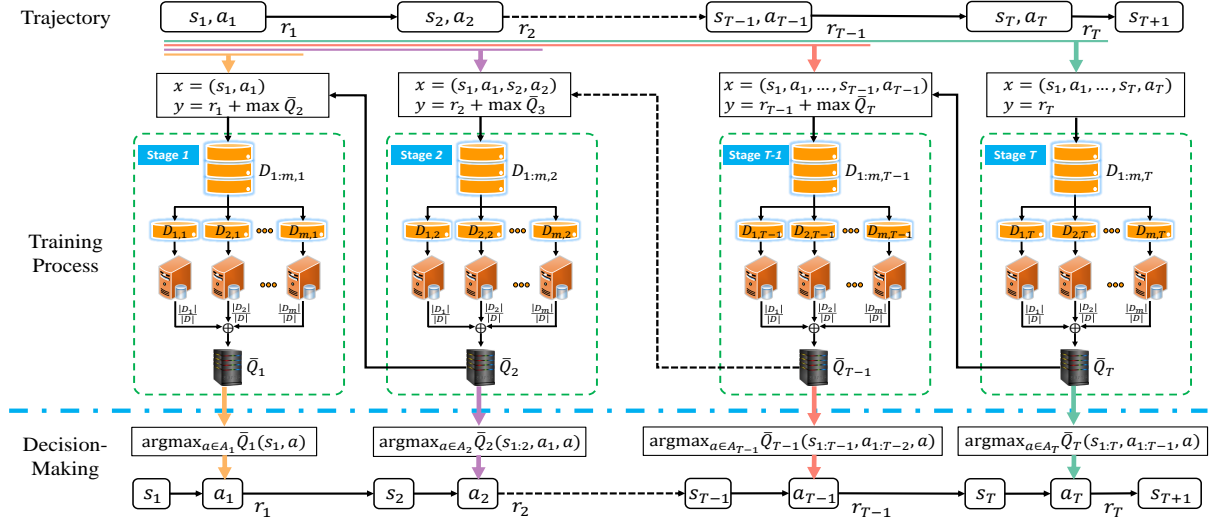
$$\bar{y}_{i,j,t} := r_{i,j,t} + \max_{a_{t+1} \in \mathcal{A}_{t+1}} \bar{Q}_{D,\lambda_{t+1},t+1}(s_{i,j,1:t+1}, a_{i,j,1:t}, a_{t+1}), \quad j = 1, \dots, m, \quad (13)$$

and run KRR with parameter λ_t on the data D_j to obtain a local estimator of the Q-function

$$Q_{D_j,\lambda_t,t} = \arg \min_{Q_t \in \mathcal{H}_{K,t}} \frac{1}{|D_j|} \sum_{i=1}^{|D_j|} (\bar{y}_{i,j,t} - Q_t(s_{i,j,1:t}, a_{i,j,1:t}))^2 + \lambda_t \|Q_t\|_{K,t}^2, \quad j = 1, \dots, m. \quad (14)$$

- *Synthesis*: Synthesize the global estimator as

$$\bar{Q}_{D,\lambda_t,t} = \sum_{j=1}^m \frac{|D_j|}{|D|} Q_{D_j,\lambda_t,t}. \quad (15)$$

Figure 2 Training and decision-making flows of DKRR-DTR.

- *Iteration and Decision-Making:* Repeat the local processing and synthesis steps for $t = T, T - 1, \dots, 1$, and obtain a set of Q-functions $\{\bar{Q}_{D,\lambda_t,t}\}_{t=1}^T$ based on DKRR. Define the DKRR for DTRs (DKRR-DTR) by $\bar{\pi}_{D,\bar{\lambda}} = (\bar{\pi}_{D,\lambda_1,1}, \dots, \bar{\pi}_{D,\lambda_T,T})$, where

$$\bar{\pi}_{D,\lambda_t,t}(s_{1:t}, a_{1:t-1}) = \arg \max_{a_t \in \mathcal{A}_t} \bar{Q}_{D,\lambda_t,t}(s_{1:t}, a_{1:t-1}, a_t), \quad t = 1, \dots, T. \quad (16)$$

The training and decision-making flows of the above approach are shown in Figure 2, where $D_{j,t}$ represents the data on the j -th local machine at the t -th stage and $\bar{Q}_{D,\lambda_t,t}$ is rewritten as \bar{Q}_t for convenience. A comparison of (15) with (9) shows that the computational complexity of KRR-DTR is reduced from $\mathcal{O}(|D|^3)$ to $\mathcal{O}(|D_j|^3)$ at each stage on the j -th local machine. If the data subset sizes are the same, then each local machine has only $\mathcal{O}(|D|^3/m^3)$ floating computations at each stage. As in the classical regression setting (Zhang et al. 2015, Lin et al. 2017), the number of local machines m balances the generalization error and computational complexity of DKRR-DTR. A small m yields perfect generalization but needs huge computations, whereas a large m significantly accelerates the algorithm but may degrade its generalization performance. Therefore, it is crucial to theoretically derive some values of m with which DKRR-DTR performs similarly to KRR-DTR while reducing its computational burden.

4. Theoretical Behaviors

According to the “no free lunch” theory (Györfi et al. 2006, Theorem 3.1), satisfactory generalization error bounds cannot be derived for learning algorithms without any assumptions about the data. Therefore, some restrictions on the data D and the distribution P should be set for our analysis. Our first assumption is mild under our setting.

ASSUMPTION 1. *For any $t = 1, \dots, T$, \mathcal{S}_t is a compact set, \mathcal{A}_t is a finite set, and there exists an $M \geq 1$ such that $\|R_t\|_{L^\infty} \leq M$ for any $t = 1, \dots, T$.*

Given Assumption 1, it is easy to check that $\mathcal{X}_t = \mathcal{S}_{1:t} \times \mathcal{A}_{1:t}$ is also compact. According to (4) and $Q_{T+1}^* = 0$, Assumption 1 implies that

$$|y_t^*| \leq (T - t + 1)M, \quad \|Q_t^*\|_{L^\infty} \leq (T - t + 1)M \quad (17)$$

hold almost surely for any $1 \leq t \leq T$, showing that the optimal Q -functions are bounded. Our second assumption focuses on the conditional probability of choosing actions.

ASSUMPTION 2. *Let $\mu \geq 1$ be a constant. It holds that*

$$p_t(a|s_{1:t}, a_{1:t-1}) \geq \mu^{-1}, \quad \forall a \in \mathcal{A}_t, t = 1, \dots, T. \quad (18)$$

Assumption 2, which has been widely used in RL (Murphy 2005b, Goldberg and Kosorok 2012), declares that conditioned on previous treatment information, any action in the finite set \mathcal{A}_t can be chosen with a probability of at least μ^{-1} . Based on Assumption 2, it follows from (Goldberg and Kosorok 2012, Eq. (16)) that for an arbitrary $Q_t \in \mathcal{L}_t^2$, there holds

$$E[V_1^*(S_1) - V_{\pi,1}(S_1)] \leq \sum_{t=1}^T 2\mu^{t/2} \sqrt{E[(Q_t - Q_t^*)^2]} = \sum_{t=1}^T 2\mu^{t/2} \|Q_t - Q_t^*\|_{\mathcal{L}_t^2}, \quad (19)$$

where $\pi = (\pi_1, \dots, \pi_T)$ is defined by $\pi_t(s_{1:t}, a_{1:t-1}) = \arg \max_{a_t \in \mathcal{A}_t} Q_t(s_{1:t}, a_{1:t-1}, a_t)$.

Our third assumption is the standard regularity assumption on Q_t^* that has been adopted in (Caponnetto and De Vito 2007, Lin et al. 2017). We first define an integral operator from $\mathcal{H}_{K,t}$ to $\mathcal{H}_{K,t}$ (also from \mathcal{L}_t^2 to \mathcal{L}_t^2 if no confusion is made) as $L_{K,t}f(x) = \int_{\mathcal{X}_t} f(x')K(x, x')dP_t(x')$. For any positive-definite kernel $K(\cdot, \cdot)$, define $L_{K,t}^r$ as the r -th power of $L_{K,t}$ via spectral calculus.

ASSUMPTION 3. For any $t = 1, \dots, T$, assume that

$$Q_t^* := L_{K,t}^r h_t, \quad \text{for some } h_t \in \mathcal{L}_t^2, \quad r > 0. \quad (20)$$

The index r in (20) quantifies the regularity of Q_t^* . If $r = 0$, then (20) means $Q_t^* \in \mathcal{L}_t^2$, implying that there is no regularity of Q_t^* . If $r = 1/2$, then (20) is equivalent to $Q_t^* \in \mathcal{H}_{K,t}$, showing that Q_t^* is in the RKHS associated with the kernel K . If $r > 1/2$, then (20) implies that Q_t^* is in other RKHSs corresponding to smoother kernels than K . Generally speaking, the larger the r value, the better the assumed regularity of Q_t^* . As indicated by (4), the regularity assumption of Q_t^* depends on the regularity of the reward function R_t . Since R_t in a DTR can be manually set before the learning process, the regularity of Q_t^* in Assumption 3 indeed includes a wide range of selection of R_t , including both the smooth and constant reward functions, and is much looser than the assumptions in existing literature (Murphy 2005b, Goldberg and Kosorok 2012, Oh et al. 2022), where Q_t^* is assumed to belong to linear spaces.

For any t , define the effective dimension (Caponnetto and De Vito 2007) as $\mathcal{N}_t(\lambda) := \text{Tr}((\lambda I + L_{K,t})^{-1} L_{K,t})$ for $\lambda > 0$, where $\text{Tr}(L)$ is the trace of the operator L . Our final assumption describes the property of K via the effective dimension.

ASSUMPTION 4. There exists an $s \in (0, 1]$ such that

$$\mathcal{N}_t(\lambda) \leq C_0 \lambda^{-s}, \quad \forall t = 1, 2, \dots, T, \quad (21)$$

where $C_0 \geq 1$ is a constant independent of λ .

From the definition of $\mathcal{N}_t(\lambda)$, (21) always holds for $C_0 = \kappa := \max_{t=1, \dots, T} \sqrt{\sup_{x \in \mathcal{X}_t} K(x, x)}$ and $s = 1$. Therefore, without this assumption, our results below always hold for $s = 1$. This assumption is introduced to encode the property of the kernel in our theoretical analysis to make the established generalization error bounds more delicate and has been utilized in studies on kernel learning (Lin et al. 2017, Lin and Zhou 2018).

In summary, four assumptions concerning D , P_t , Q_t^* , and K are involved in our analysis. These assumptions can be simultaneously satisfied easily. For example, assume the state space is $\mathcal{S}_t := [0, 1]$

and the action space is $\{0, 1\}$; conditioned on $s_{1:t}, a_{1:t-1}$, one adopts the decision $a_t = 1$ with probability $1/2$ and the reward function $R_t(x) \equiv C$ for some constant C . If we adopt the Sobolev kernel $K(x_t, x'_t) = \max\{x_t \cdot x'_t, 1 - x_t \cdot x'_t\}$, then the above assumptions hold simultaneously with $\mu = 2$, $M = C$, $r = 1$, and $s = 1$. Based on the above assumptions, we bound the generalization error of KRR-DTR to show the power of kernel-based Q-learning in the following theorem.

THEOREM 1. *Under Assumptions 1-4, with $\frac{1}{2} \leq r \leq 1$ and $0 < s \leq 1$, if $\lambda_1 = \dots = \lambda_T = |D|^{-\frac{1}{2r+s}}$, then*

$$E \left[V_1^*(S_1) - V_{\pi_{D, \lambda}, 1}(S_1) \right] \leq C_1(T, \mu) |D|^{-\frac{r}{2r+s}}, \quad (22)$$

where $C_1(T, \mu) := C_1(2\mu\bar{C})^T T \sum_{t=1}^T 2^{-t} \sum_{\ell=t}^T \prod_{k=\ell}^{T-1} ((T-k+2)(2\mu^{1/2})^{k-\ell} + 1)$, and \bar{C} and C_1 are constants depending only on M , C_0 , κ , r , s , and $\max_{t=1, \dots, T} \|h_t\|_{\mathcal{L}_t^2}$.

Theorem 1 quantifies the relation between prediction accuracy of KRR-DTR and the data size. According to (22), the generalization error of KRR-DTR decreases with respect to the data size. Moreover, it depends heavily on the regularity of the optimal Q-functions and the property of the adopted kernel. In particular, the better the regularity of Q_t^* , the smaller the generalization error; the smaller the effective dimension of the kernel, the better the quality of KRR-DTR. The derived rate $\mathcal{O}(|D|^{-\frac{r}{2r+s}})$ is the same as that for the classical KRR for regression in supervised learning (Caponnetto and De Vito 2007, Lin et al. 2017) under similar assumptions. The derived generalization error is dimensionality independent, showing that using kernel methods in Q-learning is essentially better than linear approaches.

In Theorem 1, the constant $C_1(T, \mu)$ behaves exponentially with respect to the horizon T , which is different from the results in (Fan et al. 2020). The main reason is that, except for the mild restriction in Assumption 2, we do not impose any restrictions on the distribution P , unlike (Fan et al. 2020). This property makes our analysis suitable only for Q-learning with a small T , coinciding with the practical implementation requirements of DTR in Table 1. Additional restrictions on P , such as the concentration-type assumption in (Fan et al. 2020) and margin-type assumption in (Oh

et al. 2022), can improve the constant $C_1(T, \mu)$ and the convergence rate $|D|^{-\frac{r}{2r+s}}$. However, as these assumptions are difficult to satisfy in practice, we do not use them in the present paper.

The derived generalization error bounds in (22) are much better than those for linear Q-learning (Murphy 2005b, Oh et al. 2022) in three aspects. First, we only impose the regularity assumption (20) on optimal Q-functions, whereas (Murphy 2005b) and (Oh et al. 2022) required Q_t^* to belong to a linear combination of finite basis functions. Second, the derived convergence rate $|D|^{-r/(2r+s)}$ is better than those established for linear Q-learning in previous studies, where rates slower than $|D|^{-1/4}$ were derived under stricter assumptions. For sufficiently small values of s , our derived rates can be of the order $|D|^{-1/2}$. Finally, due to linearity, the rates established in (Murphy 2005b) and (Oh et al. 2022) depend heavily on the dimension d , whereas our results are dimensionality independent, showing the power of kernelization.

Our next theoretical result presents a solid theoretical guarantee for the feasibility of DKRR-DTR.

THEOREM 2. *Under Assumptions 1-4, with $\frac{1}{2} \leq r \leq 1$ and $0 < s \leq 1$, if $\lambda_1 = \dots = \lambda_T = |D|^{-\frac{1}{2r+s}}$, $|D_1| = \dots = |D_m|$, and*

$$m(\log m + 1) \leq \frac{|D|^{\frac{2r+s-1}{4r+2s}}}{\log |D|}, \quad (23)$$

then

$$E \left[V_1^*(S_1) - V_{\bar{\pi}_{D, \vec{\lambda}}, 1}(S_1) \right] \leq C_2(T, \mu) |D|^{-\frac{r}{2r+s}}, \quad (24)$$

where $C_2(T, \mu) := C_2(2\mu\hat{C})^T T \sum_{t=1}^T 2^{-t} \sum_{\ell=t}^T \prod_{k=\ell}^{T-1} ((T-k+2)(2\mu^{1/2})^{k-\ell} + 1)$, and \hat{C} and C_2 are constants depending only on M , C_0 , κ , r , s , and $\max_{t=1, \dots, T} \|h_t\|_{\mathcal{L}_t^2}$.

Theorem 2 presents a sufficient condition of m to guarantee the excellent generalization performance of DKRR-DTR. In particular, if the number of data subsets m and the total number of samples $|D|$ satisfy the relation (23), then DKRR-DTR performs almost the same as KRR-DTR, showing that the computation reduction approach made by distributed learning does not degrade the generalization performance of KRR-DTR. The restriction on m , such as (23), is necessary because the generalization performance of KRR-DTR cannot be realized if we use DKRR-DTR with each data subset containing only a few samples.

Theorem 2 shows that DKRR-DTR possesses all the advantages of KRR-DTR, but its training cost is only $\mathcal{O}(|D|^3/m^3) \times m = \mathcal{O}(|D|^3/m^2)$, which is $1/m^2$ times smaller than that of KRR-DTR. Given that the quality of Q-learning algorithms is measured by their generalization performance, computational costs, and stability, the above assertions show that DKRR-DTR is better than linear Q-learning in generalization, better than deep Q-learning and KRR-DTR in computation, and better than deep Q-learning in stability as the optimization model defined by (14) can be analytically solved, whereas obtaining global minima with high-quality deep neural networks remains an open question in the realm of deep learning (Goodfellow et al. 2016, Chap.8). These findings illustrate that DKRR-DTR is a promising approach to yielding high-quality DTRs.

5. Simulations

In this section, two types of clinical trials for cancer treatment are simulated to demonstrate the efficacy of the proposed method compared with fitted-Q-iteration methods, where the hypothesis spaces for Q-function approximation are linear spaces and deep neural networks, denoted by LS-DTR and DNN-DTR, respectively, as well as several commonly used policy gradient-related methods, which include policy gradient (PG) (Sutton et al. 1999), actor-critic (AC) (Mnih et al. 2016), soft actor-critic (SAC) (Haarnoja et al. 2019), proximal policy optimization (PPO) (Schulman et al. 2017), deep deterministic policy gradient (DDPG) (Lillicrap et al. 2016), and twin-delayed deep deterministic (TD3) policy gradient (Fujimoto et al. 2018). Additionally, we compare the proposed method with several offline methods, specifically model-based policy optimization (MBPO) (Janner et al. 2019), using base agents PPO, DDPG and TD3, respectively. For a fair comparison, we clarify some implementation details in the following:

- In fitted-Q-iteration, consistent hyperparameter values are maintained across clinical stages.

Kernel-based Q-learning employs the Gaussian kernel. DKRR-DTR distributes training samples randomly and equally across local machines. DNN-DTR utilizes a fully connected feedforward network with sigmoid activation and Xavier initialization (Glorot and Bengio 2010).

- For PG-related methods, a fully connected feedforward neural network with the ReLU activation function and Kaiming initialization (He et al. 2015) is employed to approximate both the policy and value functions.

- For MBPO methods, we first train an environment model using offline experiences. This involves training DNNs to approximate transition, reward, and terminal functions. Here, we use three transition functions as an ensemble of transition models to generate experiences. Subsequently, we update the actor and critic using the experiences generated by the trained environment model.

All simulations are run on a desktop workstation equipped with an Intel(R) Core(TM) i9-10980XE 3.00 GHz CPU, an Nvidia GeForce RTX 3090 GPU, 128 GB of RAM, and Windows 10; the DNN-DTR programs are executed on the GPU, and the others are executed on the CPU. The results are recorded by averaging the results from multiple individual trials with the best parameters.

5.1. Clinical trial with a small number of treatment options

NSCLC patients typically receive 1-3 treatment lines, flexible depending on disease progression and therapy tolerance. This simulation aims to develop an optimal treatment policy that maximizes the expected survival time. We use the cancer dynamics model by Goldberg and Kosorok (2012) with aggressive (A) and conservative (B) treatments to generate the clinical trajectory. Trajectory generation details are given in the appendix. The following cases are considered to examine the performance of the proposed method:

- Single feature + Separately (S+S): The state is the wellness at the start of the current stage, and the Q-functions are estimated separately for actions A and B .
- Multiple feature + Separately (M+S): The state is comprised of the wellness at the start of the current stage and the reward obtained from the previous stage. The Q-functions are estimated separately for actions A and B .
- Multiple feature + Jointly (M+J): The state is the same as in the case of M+S, and the Q-function is estimated to be a joint function of the state and action.
- Non-Markovian + Jointly (N+J): The state is the same as in the case of M+S, and the Q-function is estimated to be a joint function of all state-action pairs across all stages up to the current one.

We generate a dataset of $N = 10000$ trajectories for training and test the policy $\pi = (\pi_1, \pi_2, \pi_3)$ by generating 1000 new trajectories in which the treatment of the i -th stage accords with π_i . Eight

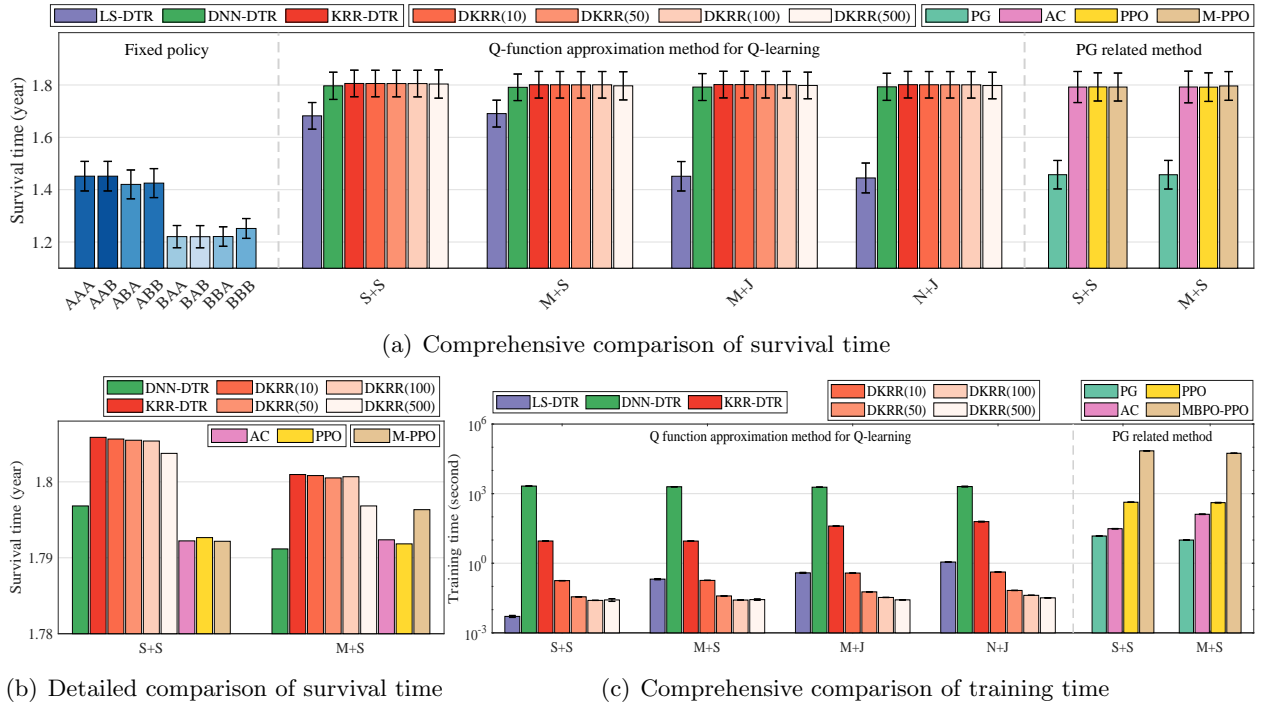


Figure 3 Comparisons of Survival time and training time for the mentioned methods

fixed treatments, where $\pi = (a_1, a_2, a_3)$ for $a_i \in \{A, B\}$, are used for baseline. For KRR-DRT and DKRR-DRT, the regularization parameter λ is chosen from the set $\{\frac{1}{2^q} | \frac{1}{2^q} > \frac{1}{2N}, q = 0, 1, 2, \dots\}$, and the kernel width σ is chosen from a set of 20 values drawn in an equally spaced logarithmic interval $[0.001, 1]$. For DNN-DRT and PG-related methods, the number of hidden layers and the neuron number in each hidden layer are chosen from the sets $\{1, 2, 3, 4\}$ and $\{10, 20, \dots, 100\}$, respectively. Additionally, the number of training epochs for DNN-DRT and the maximum number of episodes for PG-related methods are both chosen from the set $\{2000, 4000, \dots, 10000\}$. The expected value of survival time is estimated using the mean of the survival time of the 1000 patients. For each method with the best parameters, we conduct the simulation 500 times and record the average value of the estimated mean survival time for evaluation.¹

The comprehensive comparisons of survival time and training time are illustrated in Figure 3, where Figure 3(b) offers a more detailed examination of the survival times among several policies that exhibit closely comparable performance. DKRR-DTR is abbreviated as DKRR for brevity and

¹ The DNN-DTR and PG-related methods are conducted 100 times because of the high training cost.

the numbers in brackets after the notation DKRR are the numbers of local machines. MBPO using base agents PPO is abbreviated as M-PPO. It should be noted that, when dealing with discrete action spaces, the PPO algorithm calculates the Q-functions separately for each individual action. Furthermore, the identity of the Q-function across all stages necessitates that the state dimensions remain the same at each stage, thus eliminating the non-Markovian case. Consequently, the PPO algorithm involves only two cases regarding the state space: the previously defined single feature and multiple feature, denoted as PPO(S) and PPO(M), respectively. From the above results, we can conclude the following: 1) The policies AAA and AAB have the best survival time among the eight fixed treatments, but they are still significantly worse than the policies obtained by RL methods, which illustrates the power of RL in discovering effective regimens. 2) Apart from DKRR-DTR, LS-DTR has the shortest training time, which increases from case S+S to case N+J. This is because the training complexity of LS-DTR is proportional to the cube of the data dimension (the dimension increases from case S+S to case N+J). Nevertheless, LS-DTR has the worst survival time among all RL methods. The survival times of LS-DTR for cases S+S and M+S are obviously higher than those of LS-DTR for cases M+J and N+J, which indicates that LS is not good at jointly handling states and actions when the size of the action space is small. 3) KRR-DTR exhibits the best performance in survival time. Although KRR-DTR does not demonstrate a notable advantage in training time compared to PG, AC, and PPO, it is crucial to highlight that the training procedures of PG, AC, and PPO necessitate direct interaction with the real environment, rendering them impractical for medical diagnosis applications where safety requirements are exceptionally rigorous. This is due to the potential for any exploratory treatment to cause irreparable harm to patients. 4) M-PPO attains comparable survival time outcomes to KRR-DTR by developing an environmental model that circumvents direct interaction with the real environment. However, training the environmental model is extremely time-consuming, requiring training times that are thousands of times longer than that of KRR-DTR. Regarding DNN-DTR, which also eliminates direct interaction with the real environment, its time cost is significantly higher-ranging from tens to hundreds of times

greater-than that of KRR-DTR, due to the necessity of training a deep neural network at each stage. 5) DKRR-DTR maintains almost equivalent performance to KRR-DTR regarding survival time. Even with 500 local machines, the performance of DKRR-DTR remains superior to that of DNN-DTR and PG-related methods. However, in terms of training time, the framework based on distributed computing significantly reduces the training time of KRR-DTR. When the number of local machines is larger than 10, the training time of DKRR-DTR (in all cases except S+S) is even less than that of LS-DTR, whose training complexity is independent of training data size. Overall, DKRR-DTR is highly efficient in the training stage while generalizing comparably to state-of-the-art methods, which implies that DKRR-DTR can be applied to large-scale DTR problems.

5.2. Clinical trial with a large number of treatment options

This simulation considers a fixed-length clinical trial with monthly treatment stages. Each patient receives a treatment at the start of each month. We design an optimal strategy balancing drug efficacy and toxicity to maximize cumulative survival probability (CSP) after all courses. The model proposed by Zhao et al. (2009) is used to generate clinical data. Details are in the appendix. Note that the action space is continuous in this simulation. The aforementioned PG-related methods are capable of directly handling such continuous action spaces. However, for fitted Q-iteration methods such as LS-DTR, DNN-DTR, and KRR-DTR, we must discretize the continuous action space into numerous dose levels. Consequently, the following cases are the sole focus of our consideration:

- Markovian + Jointly (M+J): The state consists of the toxicity and tumor size at the current stage, and the Q-function is estimated to be a joint function of the state and action.
- Non-Markovian + Jointly (N+J): The state is the same as in the case of M+J, and the Q-function is estimated to be a joint function of all state-action pairs across all stages up to the current stage.

Note that PG-related methods calculate the Q-functions as a combined function of both the state and action, and the identity of the Q-function across all stages negates the non-Markovian case.

The settings of this simulation are as follows. We generate $N = 20000$ trajectories for training and 1000 trajectories for evaluation. Ten fixed treatments whose dose levels range from 0.1 to 1.0

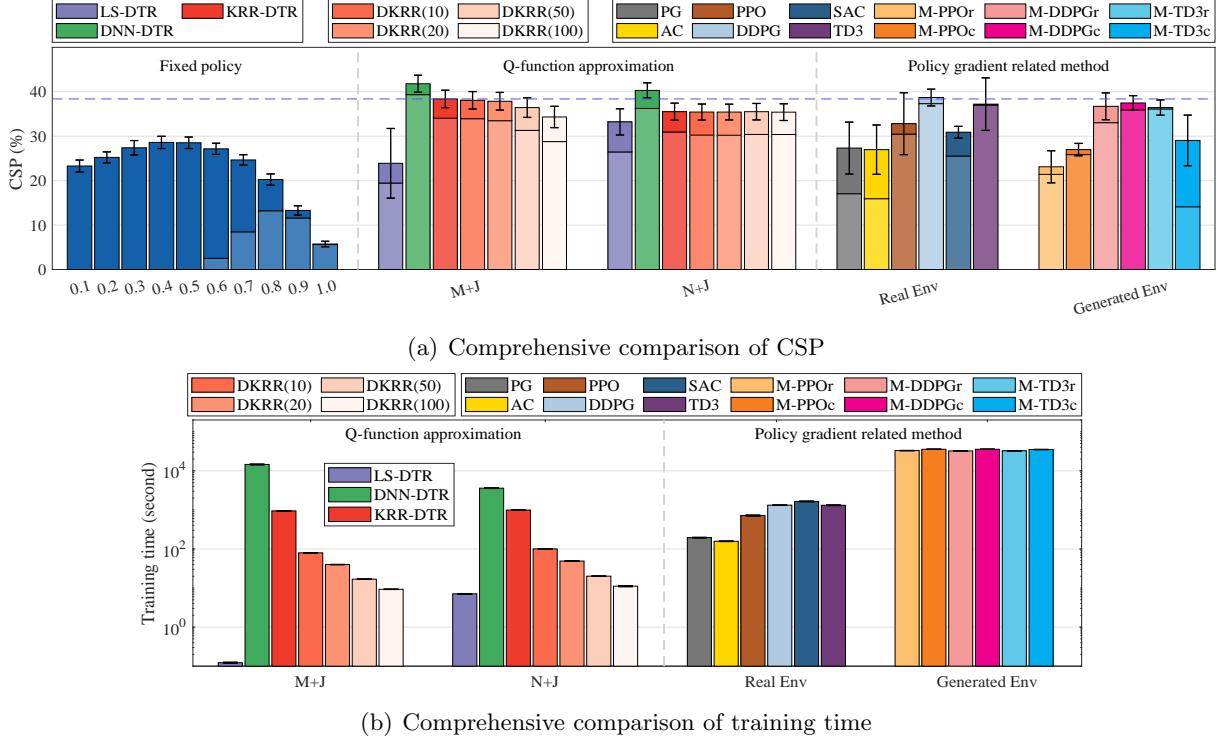


Figure 4 Comparisons of CSP and training time for the mentioned methods.

in increments of 0.1 are used for baselines. For KRR-DRT and DKRR-DRT, λ is chosen from the set $\{\frac{1}{2^q} | \frac{100}{N} > \frac{1}{2^q} > \frac{1}{10N}, q = 0, 1, 2, \dots\}$, and the kernel width σ is chosen from a set of 20 values drawn in an equally spaced logarithmic interval $[0.01, 10]$. The parameter ranges for DNN-DRT and PG-related methods follow Section 5.1. The expected CSP value is estimated using the mean CSP value of the 1000 patients. The simulation is conducted 100 times for each method with the best parameters, and the average value of the estimated mean CSP is reported.²

Comparisons of the CSP and training time are shown in Figure 4, where the light and dark shades of each color series represent the cumulative cured probability (CCP) and trial end probability (TEP) of the compared methods, respectively. The dashed blue line depicted in Figure 4(a) signifies the CSP of KRR-DTR in the case of M+J. In MBPO methods, the suffix ‘c’ and ‘r’ denote the utilization of classification and regression techniques, respectively, for the construction of the reward model. Here, the CCP is the proportion of patients cured in the treatment cycle, and TEP is the

² The DNN-DTR and PG-related methods are conducted 20 times.

proportion of patients alive but not cured at the end of the trial. From the results, we obtain the following observations: 1) Some fixed treatments, such as dose levels of 0.3 – 0.6, have good CSP values and even outperform LS-DTR in the case of M+J. However, their CCP values are evidently lower than those of Q-learning methods. The CCP is usually more important than TEP because patients prefer to be cured in the treatment cycle. Hence, RL can provide effective treatment policies for life-threatening diseases. 2) DNN-DTR performs the best because of its excellent nonlinear fitting capability for Q-functions, but its training is very time-consuming. LS-DTR has the shortest training time; the CSP value of LS-DTR in the case of N+J is significantly better than that in M+J due to the expansion of the linear hypothesis space (the dimension of data input grows with the number of stages in N+J), but LS-DTR still has the lowest CSP values and the highest standard deviations. 3) The training time of PG-related methods that interact with the real environment primarily depends on the number of episodes, and it is either comparable to or superior to that of KRR-DTR. Despite that DDPG, a method within this category, achieves superior performance on CSP compared to KRR-DTR, such methods are unsuitable for application in medical diagnosis due to their inability to meet the extremely high safety requirements. MBPO methods do not require interaction with the real environment during training and demonstrate nearly equivalent performance to KRR-DTR in terms of CSP. However, the necessity to train an environmental model significantly prolongs their overall training time compared to all other methods. 4) KRR-DTR is a compromise between the CSP and training time; its CSP value is slightly smaller than that of DNN-DTR, but it is more efficient than DNN-DTR and MBPO methods. More importantly, it possesses the capability of offline training, a feature that fully meets the stringent requirements for safety. By distributing data across multiple local machines, DKRR-DTR effectively circumvents the limitations of KRR-DTR in handling large-scale data training. Its parallel computing capability significantly reduces the training time, while maintaining comparable performance levels to KRR-DTR in terms of CSP.

These simulations illustrate that DKRR-DTR has higher efficiency and superior performance in dealing with large-scale DTR problems compared with state-of-the-art methods.

6. Conclusion

This paper introduced a distributed Q-learning algorithm that integrates DKRR with Q-learning to mitigate the computational burden associated with DTRs. Through the development of a novel integral operator, we established tight generalization error bounds for the proposed algorithm within the framework of statistical learning theory. Our theoretical findings indicate that the distributed operator does not compromise the generalization error, provided that the data are not excessively fragmented into numerous subsets. Furthermore, the derived error bounds are independent of the data dimension, implying that the proposed algorithm scales effectively with respect to the problem's dimensions. In addition to our theoretical analysis, we also applied the proposed algorithm to two types of clinical trials for cancer treatment, including those aimed at increasing survival time and CSP. The numerical results verify our theoretical assertions and demonstrate the feasibility and efficiency of the proposed algorithm in applications.

Acknowledgments

We are deeply grateful to Professor Shaojie Tang for his insightful suggestions and significant contributions to this work. The work of this paper is partially supported by National Natural Science Foundation of China (Grant Nos. 12471486,12371513,2276209).

Appendix A: Introduction of Simulation 1

This section provides a thorough description of the trajectory data production for Section 5.1. The observation period for patients in the clinical trial is 5 years. At each time point $t \in [0, 5]$, the tumor size denoted by $M(t)$ and the wellness denoted by $W(t)$ for each patient are recorded. When a patient's wellness is less than 0.2, the patient suffers from death. When a patient's tumor size reaches 1, treatment should be administered. Here, an aggressive treatment (denoted by A) or a conservative treatment (denoted by B) is considered for application to patients. The immediate effects on wellness and tumor size for the two treatments are formulated as

$$W(t_i^+|A) = W(t_i) - 0.5, \quad M(t_i^+|A) = 0.1M(t_i)/W(t_i),$$

$$W(t_i^+|B) = W(t_i) - 0.25, \quad M(t_i^+|B) = 0.2M(t_i)/W(t_i).$$

It can be seen that the aggressive treatment A yields a greater decrease in tumor size and wellness than the conservative treatment B . In the following, we rewrite both of $W(t_i^+|A)$ and $W(t_i^+|B)$ as $W(t_i^+)$, and rewrite both of $M(t_i^+|A)$ and $M(t_i^+|B)$ as $M(t_i^+)$ for convenience. With the treatment, a patient's current survival time τ_i is drawn independently according to an exponential distribution, with a mean of $0.15(W(t_i^+) + 2)/M(t_i^+)$.

The cancer dynamics after t_i satisfy the following equations:

$$W(t) = W(t_i^+) + (1 - W(t_i^+))(1 - 2^{-(t-t_i)/2}), \quad M(t) = M(t_i^+) + 2M(t_i^+)(t - t_i).$$

Noted that the i th stage begins at time point t_i , and ends at time point t_{i+1} such that $M(t_{i+1}) = 1$ for some $t_i < t_{i+1} < 5$, or the patient dies, or the clinical trial ends. Specifically, we can obtain the critical time point $\hat{t}_i = t_i + 0.75 \left(\frac{1 - M(t_i^+)}{M(t_i^+)} \right)$ from $M(\hat{t}_i) = 1$, and thus compute the end of the i th stage via $t_{i+1} = \min\{\hat{t}_i, t_i + \tau_i, 5\}$.

We assume that only patients in urgent need of treatment are enrolled in the clinical trial, which means that all patients meet $M(0) = 1$ and thus $t_1 = 0$. The wellness of patients at the beginning of the first stage is drawn independently according to the uniform distribution in the interval $[0.5, 1]$. A treatment is randomly chosen from the set $\{A, B\}$ for each time point t_i . The reward is defined as the actual survival time of the current stage. Due to the differences in initial wellness, survival time, and treatment policies for different patients, the generated trajectories may have different numbers of stages. Here, the total number of stages for all patients is limited to 3. For the missing stages of the trajectory data with a number of stages less than 3, we fill wellness and reward as zeros and randomly choose actions from the set $\{A, B\}$ with equal probability, modifying the trajectory to a fixed length of 3.

Appendix B: Introduction of Simulation 2

This section describes the process of generating trajectory data in Section 5.2. In this simulation, patients are monitored monthly for 6 months, and treatment is applied to each patient at the beginning of each month. The relation of a drug's toxicity W_i , tumor size M_i , and drug dosage A_i of treatment is characterized by the following system of ordinary difference equations:

$$W_{i+1} = W_i + 0.1(M_i \vee M_0) + 1.2(A_i - 0.5),$$

$$M_{i+1} = (M_i + (0.15(W_i \vee W_0) - 1.2(A_i - 0.5)) \times \mathbf{1}_{M_i > 0}) \vee 0,$$

for $i = 1, \dots, 6$, where $\mathbf{1}_{M_i > 0}$ is an indicator function representing that there will be no future recurrence of the tumor when the tumor size reaches 0 (that is, the patient has been cured). The initial values of toxicity W_1 and tumor size M_1 are drawn independently according to the uniform distribution on the interval $(0, 2)$. The drug dosage treatment sets for the first stage and last five stages are $\{0.51, 0.52, \dots, 1\}$ and $\{0.01, 0.02, \dots, 1\}$, respectively. They are discretized from drug dosage intervals $(0.5, 1]$ and $(0, 1]$ with an increment of size 0.01. The action A_1 and the actions A_i ($i = 2, \dots, 6$) are randomly chosen from the sets $\{0.51, 0.52, \dots, 1\}$ and $\{0.01, 0.02, \dots, 1\}$ with equal probability, respectively. To increase the stochasticity of the survival status, we define the conditional probability of death for the i th stage as

$$p_i = 1 - \exp(-\exp(W_i + M_i - 4.5)).$$

The survival status (death is coded as 1) is drawn independently according to the Bernoulli distribution $B(p_i)$. The reward for each stage is assumed to depend on the states (including toxicity and tumor size) observed right before and after each action, and it can be decomposed into three types of rewards: $R_{i,1}(A_i, W_{i+1}, M_{i+1})$ related to survival status, $R_{i,2}(W_i, A_i, W_{i+1})$ related to toxicity change, and $R_{i,3}(M_i, A_i, M_{i+1})$ related to tumor size change. Specifically, they are defined by

$$R_{i,1}(A_i, W_{i+1}, M_{i+1}) = -6, \quad \text{if patient died,} \quad (25)$$

otherwise,

$$R_{i,2}(W_i, A_i, W_{i+1}) = \begin{cases} 0.5, & \text{if } W_{i+1} - W_i \leq -0.5, \\ -0.5, & \text{if } W_{i+1} - W_i \geq 0.5, \\ 0, & \text{if } -0.5 < W_{i+1} - W_i < 0.5, \end{cases} \quad (26)$$

$$R_{i,3}(M_i, A_i, M_{i+1}) = \begin{cases} 1.5, & \text{if } M_{i+1} = 0, \\ 0.5, & \text{if } M_{i+1} - M_i \leq -0.5 \text{ and } M_{i+1} > 0, \\ -0.5, & \text{if } M_{i+1} - M_i \geq 0.5, \\ 0, & \text{if } -0.5 < M_{i+1} - M_i < 0.5. \end{cases} \quad (27)$$

Because overall survival is the main focus of clinical interest, we take a high penalty of -6 for the death of a patient in the equation (25), and we take a relatively large bonus of 1.5 for the cure of a patient in the equation (27). In other cases, rewards are given according to the changes in toxicity and tumor size in two consecutive stages.

Appendix C: An Analysis of the Impact of Stage Number on DTR Performance

In this section, we present a comprehensive analysis of the impact of stage number T on DTR performance. To this end, we first elucidate several implementation details as follows:

- For Simulation 1, based on previous results, we select the M-PPO algorithm, which performs best among the policy gradient-related algorithms, and the best fixed policy to compare with our proposed KRR-DTR. The number of stages T varies from the set $\{3, 4, \dots, 10\}$. For each given T , the observation period for patients in the clinical trial is $T + 2$ years. The immediate effects on wellness for the two treatments are formulated as

$$W(t_i^+|A) = W(t_i) - (0.53 - 0.01T), \quad W(t_i^+|B) = W(t_i) - (0.265 - 0.005T).$$

With the treatment, a patient's current survival time τ_i is drawn independently according to an exponential distribution, with a mean of

$$(0.12 + 0.01 * T)(W(t_i^+) + 2)/M(t_i^+).$$

The tumor size after t_i satisfies the following equations:

$$M(t) = M(t_i^+) + (1.7 + 0.1T)M(t_i^+)(t - t_i).$$

The remaining parameter settings and environmental dynamics are the same as those in the manuscript.

- For Simulation 2, we choose the two most prominent methods within policy gradient approaches: DDPG and M-DDPGc for comparison with our proposed method. Furthermore, we select the optimal constant dose regimen as a benchmark for reference purposes. The number of stages T varies within the set $\{6, 8, \dots, 20\}$. For each specific stage number T , the parameter configurations and environmental dynamics remain consistent with those detailed in the manuscript.

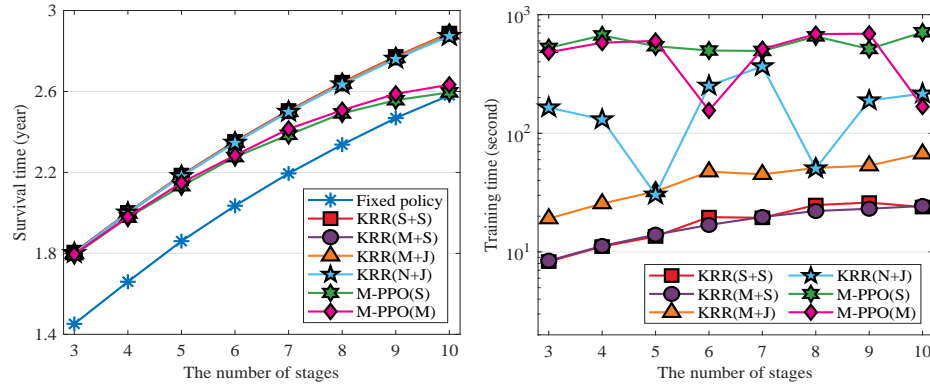


Figure 5 Comparison of survival time and training time with increasing number of stages for the methods of fixed policy, KRR-DTR, and MBPO-PPO

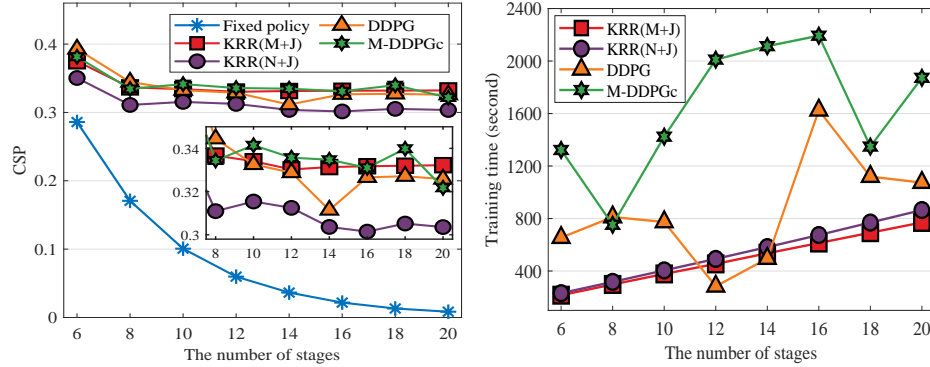


Figure 6 Comparison of CSP and training time with increasing number of stages for the methods of fixed policy, KRR-DTR, DDPG and MBPO-DDPG

- For policy gradient-related methods, in the context of both the policy network and the value network, the number of hidden layers, the neuron number in the hidden layers, and the critical threshold for terminating the training are selected from the sets $\{1, 2, 3, 4\}$, $\{10, 20, \dots, 100\}$, and $\{2000, 4000, \dots, 10000\}$, respectively.
- For each specified stage number T , we generate 10000 trajectories for training in our proposed KRR-DTR. To ensure fairness, in the context of model-based policy optimization (MBPO) related methods, we utilize 10000 episodes of data obtained through real environmental interactions to train the environment model, which includes the transition function, reward function, and terminal function. Furthermore, the maximum number of training episodes for the agents employed in policy gradient-related methods is set to 10000. All compared methods are evaluated on newly generated set of 1000 trajectories. The results are recorded by calculating the average of multiple individual trials with the best parameters.

The comparisons of the specific targets of different tasks (survival time in Simulation 1 and CSP in Simulation 2) and the training time, with an increasing number of stages for the involved methods, are shown in Figures 5-6, where KRR-DTR is abbreviated as KRR for brevity and the symbols in brackets represent the different considered cases. It should be noted that, when addressing discrete action spaces, the PPO algorithm calculates the Q-functions separately for each individual action. Moreover, the identity of the Q-function across all stages necessitates that the state dimensions remain the same at each stage, thus eliminating the non-Markovian case. Consequently, the PPO algorithm involves only two cases regarding the state space: one case where the wellness w_i serves as the sole component of the state s_i , and another where both the wellness w_i and the reward r_{i-1} obtained from the previous stage collectively constitute the state s_i . These two cases are denoted as PPO(S) and PPO(M), respectively. The DDPG algorithm calculates the Q-functions as a combined function of both the state s_i and action a_i , and the identity of the Q-function across all stages also negates the non-Markovian case. From the results, we have the following observations:

- In the task of Simulation 1, which focuses on maximizing the expected survival time, the average survival time of the compared methods consistently increases as the number of treatment stages T rises (equivalently, as the observation period $T + 2$ is extended). Although the PPO algorithm performs comparably to our proposed KRR-DTR method when the number of stages is relatively low, as the number of stages progressively increases, the superiority of PPO over fixed policy diminishes. In stark contrast, KRR-DTR demonstrates significant and consistent advantages across all stages.
- In the task of Simulation 2, which aims at maximizing the CSP after T treatment courses, the average CSP of all compared methods demonstrates a consistent decline as the number of treatment stages increases, attributed to the progressive reduction in the number of survivors. Specifically, the adoption of the fixed policy results in a particularly steep decline in CSP, forming a stark contrast with the more gradual decrease exhibited by strategies obtained through reinforcement learning. As the number of stages reaches 14 or beyond, the CSP under reinforcement learning strategies remains relatively stable, clearly showcasing the superior efficacy of reinforcement learning. In the ‘M+J’ case, KRR-DTR demonstrates performance comparable to DDPG. However, in the ‘N+J’ case, KRR-DTR is slightly inferior to DDPG, aligning with the related findings presented in the main manuscript. This may stem from the fact that the simulation experiment is grounded on the Markov assumption, rendering the use of non-Markov states inappropriate for training agents. It is noteworthy that DDPG also did not utilize non-Markov states during its training process.

- In terms of training time, these two types of tasks exhibit certain similarities. Specifically, the KRR-DTR method requires training a corresponding Q-function for each stage, thus its training time roughly increases linearly with the number of stages. Conversely, policy gradient-related methods utilize a consistent Q-function across all stages, with training time primarily contingent upon the quantity of episodes utilized in the training process. The fluctuation in training time primarily arises from the best number of episodes selected from the set $\{2000, 4000, \dots, 10000\}$, thereby preventing a proportional increase in training time with the augmentation of stages, as observed in the case of KRR-DTR. It is worth noting that, to more clearly reveal the relationship between training time and the number of stages, the time for training the environment model (both tasks take tens of thousands of seconds) is not included in the training time when considering MBPO-related methods (such as MBPO-PPO and MBPO-DDPGc). Despite this, the training time of KRR-DTR remains significantly shorter compared to that of policy gradient-based algorithms. However, given the linear relationship between the training time of KRR-DTR and the number of stages, KRR-DTR is not suitable for handling DTR tasks that involve hundreds or more stages. While DKRR-DTR can improve the training speed of KRR-DTR to a certain extent through distributed computation, its training time still exhibits a linear relationship with the number of stages. Additionally, an excessively high number of distributed nodes may adversely affect the generalization performance of DKRR-DTR.

In summary, our proposed KRR-DTR method is ideally suited for DTR tasks with a small number of stages, specifically in the tens, as shown in the above simulations. However, neither its training efficiency nor generalization performance renders it viable for DTR tasks that encompass hundreds or more stages.

Appendix D: Proofs

In this section, we develop a novel integral operator approach for Q-learning. Our main tools are error decomposition for KRR-DTR and DKRR-DTR based on their operator representations and uniform bounds for KRR-DTR and DKRR-DTR estimators.

D.1. Operator representations and differences

The core of the integral operator approach developed in (Smale and Zhou 2005, Caponnetto and De Vito 2007, Lin et al. 2017) is the operator representation of kernel-based learning algorithms, error decomposition, and tight bounds of operator differences.

For each $t = 1, \dots, T$, let $S_{D,t} : \mathcal{H}_{K,t} \rightarrow \mathbb{R}^{|D|}$ be the sampling operator defined by $S_{D,t}Q_t := (Q_t(x_{i,t}))_{i=1}^{|D|}$. Its scaled adjoint $S_{D,t}^T : \mathbb{R}^{|D|} \rightarrow \mathcal{H}_{K,t}$ is given by $S_{D,t}^T \mathbf{c} := \frac{1}{|D|} \sum_{i=1}^{|D|} c_i K_{x_{i,t}}$ for $K_x = K(x, \cdot)$ and $\mathbf{c} :=$

$(c_1, c_2, \dots, c_{|D|})^T \in \mathbb{R}^{|D|}$. Define $L_{K,D,t}Q_t := S_{D,t}^T S_{D,t} Q_t = \frac{1}{|D|} \sum_{i=1}^{|D|} Q_t(x_{i,t}) K_{x_{i,t}}$. Then, $Q_{D,\lambda_t,t}$, defined by (9), can be analytically represented as (Smale and Zhou 2005)

$$Q_{D,\lambda_t,t} = (L_{K,D,t} + \lambda_t I)^{-1} S_{D,t}^T \mathbf{y}_{D,t}, \quad (28)$$

where $\mathbf{y}_{D,t} := (y_{1,t}, \dots, y_{|D|,t})^T$. Define

$$\hat{Q}_{D,\lambda_t,t} := (L_{K,D,t} + \lambda_t I)^{-1} S_{D,t}^T \mathbf{y}_{D,t}^*, \quad Q_{D,\lambda_t,t}^\diamond := (L_{K,D,t} + \lambda_t I)^{-1} L_{K,D,t} Q_t^*, \quad (29)$$

where $\mathbf{y}_{D,t}^* = (y_{1,t}^*, \dots, y_{|D|,t}^*)^T$. Then $\hat{Q}_{D,\lambda_t,t}$ can be regarded as running KRR on the data set $\{(x_{i,t}, y_{i,t}^*)\}_{i=1}^{|D|}$, while $Q_{D,\lambda_t,t}^\diamond$ is a noise-free version of $\hat{Q}_{D,\lambda_t,t}$. Let

$$\hat{Q}_{D_j,\lambda_t,t} := (L_{K,D_j,t} + \lambda_t I)^{-1} S_{D_j,t}^T \mathbf{y}_{D_j,t}^*, \quad Q_{D_j,\lambda_t,t}^\diamond := (L_{K,D_j,t} + \lambda_t I)^{-1} L_{K,D_j,t} Q_t^* \quad (30)$$

be the corresponding local estimators for $\hat{Q}_{D,\lambda_t,t}$ and $Q_{D,\lambda_t,t}^\diamond$, respectively. Define further

$$Q_{D,\lambda_t,t}^\oplus = (L_{K,D,t} + \lambda_t I)^{-1} S_{D,t}^T \bar{\mathbf{y}}_t \quad (31)$$

as the batch version of $Q_{D,\lambda_t,t}$, where $\bar{\mathbf{y}}_t = (\bar{y}_{1,t}, \dots, \bar{y}_{|D|,t})^T$ with

$$\bar{y}_{i,t} := r_{i,t} + \max_{a_{t+1} \in \mathcal{A}_t} \bar{Q}_{D,\lambda_{t+1},t+1}(s_{i,1:t+1}, a_{i,1:t}, a_{t+1}). \quad (32)$$

It is obvious that $Q_{D,\lambda_t,t}^\oplus$ is different from $Q_{D,\lambda_t,t}$ due to their different outputs of data. Denote

$$Q_{D,\lambda_t,t}^*(x_{i,t}) := E[Y_{i,t} | X_t = x_{i,t}] = E \left[R(X_t, S_{t+1}) + \max_{a_{t+1}} Q_{D,\lambda_{t+1},t+1}(X_t, S_{t+1}, a_{t+1}) \middle| X_t = x_{i,t} \right], \quad (33)$$

and

$$\bar{Q}_{D,\lambda_t,t}^*(x_{i,t}) := E[\bar{Y}_t | X_t = x_{i,t}] = E \left[R(X_t, S_{t+1}) + \max_{a_{t+1}} \bar{Q}_{D,\lambda_{t+1},t+1}(X_t, S_{t+1}, a_{t+1}) \middle| X_t = x_{i,t} \right]. \quad (34)$$

The basic idea of our analysis is to develop novel error decomposition strategies to divide $\|Q_{D,\lambda_t,t} - Q_t^*\|_{\mathcal{L}_t^2}$ into differences among $Q_{D,\lambda_t,t}$, $Q_{D,\lambda_t,t}^\oplus$, $\hat{Q}_{D,\lambda_t,t}$, $Q_{D,\lambda_t,t}^\diamond$ and $\bar{Q}_{D,\lambda_t,t}$, which can be bounded by the difference between $L_{K,D,t}$ and $L_{K,t}$. For this purpose, write

$$\mathcal{W}_{D,\lambda_t,t} := \|(L_{K,t} + \lambda_t I)^{-1/2} (L_{K,t} - L_{K,D,t}) (L_{K,t} + \lambda_t I)^{-1/2}\|, \quad (35)$$

$$\mathcal{A}_{D,\lambda_t,t} := \|(L_{K,t} + \lambda_t I)^{1/2} (L_{K,D,t} + \lambda_t I)^{-1} (L_{K,t} + \lambda_t I)^{1/2}\|, \quad (36)$$

$$\mathcal{U}_{D,\lambda_t,t,f} := \|(L_{K,t} + \lambda_t I)^{-1/2} (L_{K,t} - L_{K,D,t}) f\|_{K,t}, \quad (37)$$

$$\mathcal{P}_{D,\lambda_t,t} := \left\| (L_{K,t} + \lambda_t I)^{-1/2} (S_{D,t}^T \mathbf{y}_{D,t}^* - L_{K,D,t} Q_t^*) \right\|_{K,t}, \quad (38)$$

$$\mathcal{S}_{D,\lambda_t,t} := \left\| (L_{K,t} + \lambda_t I)^{-1/2} (S_{D,t}^T (\mathbf{y}_{D,t}^* - \bar{\mathbf{y}}_{D,t}) - L_{K,D,t} (Q_t^* - \bar{Q}_{D,\lambda_t,t}^*)) \right\|_{K,t}, \quad (39)$$

$$\mathcal{S}_{D,\lambda_t,t} := \left\| (L_{K,t} + \lambda_t I)^{-1/2} (S_{D,t}^T (\mathbf{y}_{D,t}^* - \mathbf{y}_{D,t}) - L_{K,D,t} (Q_t^* - Q_{D,\lambda_t,t}^*)) \right\|_{K,t}. \quad (40)$$

Our road-map of proofs is to first decompose the generalization error into differences among $Q_{D,\lambda_t,t}$, $Q_{D,\lambda_t,t}^\oplus$, $\hat{Q}_{D,\lambda_t,t}$, $Q_{D,\lambda_t,t}^\diamond$, and $\bar{Q}_{D,\lambda_t,t}$, and then quantify the differences via the above terms, and finally derive tight estimates of these terms via some statistical tools.

D.2. Error decomposition for KRR-DTR

In this subsection, we present an error decomposition and then derive an oracle inequality for KRR-DTR.

Due to the triangle inequality, we get the following error decomposition directly.

PROPOSITION 1. *For any $1 \leq t \leq T$, we have*

$$\begin{aligned} & \left\| (L_{K,t} + \lambda_t I)^{1/2} (Q_{D,\lambda_t,t} - Q_t^*) \right\|_{K,t} \leq \left\| (L_{K,t} + \lambda_t I)^{1/2} (Q_{D,\lambda_t,t}^\diamond - Q_t^*) \right\|_{K,t} \\ & + \left\| (L_{K,t} + \lambda_t I)^{1/2} (Q_{D,\lambda_t,t}^\diamond - \hat{Q}_{D,\lambda_t,t}) \right\|_{K,t} + \left\| (L_{K,t} + \lambda_t I)^{1/2} (\hat{Q}_{D,\lambda_t,t} - Q_{D,\lambda_t,t}) \right\|_{K,t}. \end{aligned} \quad (41)$$

We call the three terms on the right-hand side of (41) as the approximation error, sample error, and multi-stage error, respectively. The approximation error, together with some regularity of the optimal Q-functions, describes the approximation capability of the RKHS $\mathcal{H}_{K,t}$. The sample error quantifies the gap between KRR with the theoretically optimal outputs Q_t^* and KRR with noisy optimal outputs y_t^* . The multi-stage error, exclusive to Q-learning, shows the difficulty of Q-learning in circumventing its multi-stage nature. The bounds of approximation error and sample error are standard and can be derived via the recently developed integral operator approach in (Blanchard and Krämer 2016, Guo et al. 2017, Lin et al. 2020).

LEMMA 1. *Under Assumption 3 with $\frac{1}{2} \leq r \leq 1$, we have*

$$\left\| (L_{K,t} + \lambda_t I)^{1/2} (Q_{D,\lambda_t,t}^\diamond - Q_t^*) \right\|_{K,t} \leq \lambda_t^r \mathcal{A}_{D,\lambda_t,t} \|h_t\|_{\mathcal{L}_t^2}, \quad \forall t = 1, \dots, T. \quad (42)$$

Proof. For any $t = 1, \dots, T$, (29) implies

$$Q_{D,\lambda_t,t}^\diamond - Q_t^* = -((L_{K,D,t} + \lambda_t I)^{-1} L_{K,D,t} - I) Q_t^* = -\lambda_t (L_{K,D,t} + \lambda_t I)^{-1} Q_t^*.$$

Then it follows from (36), Assumption 3, $\|Af\|_K \leq \|A\| \|f\|_K$ for positive operator A , and the fact $\left\| L_{K,t}^{1/2} f \right\|_{K,t} = \|f\|_{\mathcal{L}_t^2}$ that

$$\begin{aligned} & \left\| (L_{K,t} + \lambda_t I)^{1/2} (Q_{D,\lambda_t,t}^\diamond - Q_t^*) \right\|_{K,t} \leq \lambda_t \left\| (L_{K,t} + \lambda_t I)^{1/2} (L_{K,D,t} + \lambda_t I)^{-1} (L_{K,t} + \lambda_t I)^{r-1/2} \right\| \left\| L_{K,t}^{1/2} h_t \right\|_{K,t} \\ & \leq \lambda_t^r \left\| (L_{K,t} + \lambda_t I)^{1/2} (L_{K,D,t} + \lambda_t I)^{-1} (L_{K,t} + \lambda_t I)^{1/2} \right\| \|h_t\|_{\mathcal{L}_t^2} \leq \lambda_t^r \mathcal{A}_{D,\lambda_t,t} \|h_t\|_{\mathcal{L}_t^2}. \end{aligned}$$

This completes the proof of Lemma 1. \square

LEMMA 2. For any $t = 1, \dots, T$, it holds that

$$\left\| (L_{K,t} + \lambda_t I)^{1/2} (Q_{D,\lambda_t,t}^\diamond - \hat{Q}_{D,\lambda_t,t}) \right\|_{K,t} \leq \mathcal{A}_{D,\lambda_t,t} \mathcal{P}_{D,\lambda_t,t}. \quad (43)$$

Proof. For any $t = 1, \dots, T$, it follows from (29) that

$$\hat{Q}_{D,\lambda_t,t} - Q_{D,\lambda_t,t}^\diamond = (L_{K,D,t} + \lambda_t I)^{-1} (S_{D,t}^T \mathbf{y}_{D,t}^* - L_{K,D,t} Q_t^*).$$

Then, (36), (38), and $\|Af\|_K \leq \|A\| \|f\|_K$ for positive operator A yield

$$\begin{aligned} & \left\| (L_{K,t} + \lambda_t I)^{1/2} (Q_{D,\lambda_t,t}^\diamond - \hat{Q}_{D,\lambda_t,t}) \right\|_{K,t} \\ & \leq \left\| (L_{K,t} + \lambda_t I)^{1/2} (L_{K,D,t} + \lambda_t I)^{-1} (L_{K,t} + \lambda I)^{1/2} \right\| \left\| (L_{K,t} + \lambda I)^{-1/2} (S_{D,t}^T \mathbf{y}_{D,t}^* - L_{K,D,t} Q_t^*) \right\|_{K,t} \\ & \leq \mathcal{A}_{D,\lambda_t,t} \mathcal{P}_{D,\lambda_t,t}. \end{aligned}$$

This completes the proof of Lemma 2. \square

The bounding of the multi-stage error is more sophisticated, as collected in the following lemma.

LEMMA 3. Under Assumption 2, for any $t = 1, \dots, T$, it holds that

$$\begin{aligned} & \left\| (L_{K,t} + \lambda_t I)^{1/2} (Q_{D,\lambda_t,t} - \hat{Q}_{D,\lambda_t,t}) \right\|_{K,t} \\ & \leq \mathcal{A}_{D,\lambda_t,t} \mathcal{S}_{D,\lambda_t,t} + \mathcal{A}_{D,\lambda_t,t} \mathcal{U}_{D,\lambda_t,t, Q_t^* - Q_{D,\lambda_t,t}^*} + \mu^{1/2} \mathcal{A}_{D,\lambda_t,t} \|Q_{D,\lambda_{t+1},t+1} - Q_{t+1}^*\|_{\mathcal{L}_{t+1}^2}. \end{aligned} \quad (44)$$

Proof. Due to (28) and (29), we have

$$\begin{aligned} & \left\| (L_{K,t} + \lambda_t I)^{1/2} (Q_{D,\lambda_t,t} - \hat{Q}_{D,\lambda_t,t}) \right\|_{K,t} = \left\| (L_{K,t} + \lambda_t I)^{1/2} (L_{K,D,t} + \lambda_t I)^{-1} S_{D,t}^T (\mathbf{y}_{D,t}^* - \mathbf{y}_{D,t}) \right\|_{K,t} \\ & \leq \left\| (L_{K,t} + \lambda_t I)^{1/2} (L_{K,D,t} + \lambda_t I)^{-1} (S_{D,t}^T (\mathbf{y}_{D,t}^* - \mathbf{y}_{D,t}) - L_{K,D,t} (Q_t^* - Q_{D,\lambda_t,t}^*)) \right\|_{K,t} \\ & \quad + \left\| (L_{K,t} + \lambda_t I)^{1/2} (L_{K,D,t} + \lambda_t I)^{-1} (L_{K,D,t} - L_{K,t}) (Q_t^* - Q_{D,\lambda_t,t}^*) \right\|_{K,t} \\ & \quad + \left\| (L_{K,t} + \lambda_t I)^{1/2} (L_{K,D,t} + \lambda_t I)^{-1} L_{K,t} (Q_t^* - Q_{D,\lambda_t,t}^*) \right\|_{K,t}. \end{aligned} \quad (45)$$

It follows from (36) and (40) that

$$\left\| (L_{K,t} + \lambda_t I)^{1/2} (L_{K,D,t} + \lambda_t I)^{-1} (S_{D,t}^T (\mathbf{y}_{D,t}^* - \mathbf{y}_{D,t}) - L_{K,D,t} (Q_t^* - Q_{D,\lambda_t,t}^*)) \right\|_{K,t} \leq \mathcal{A}_{D,\lambda_t,t} \mathcal{S}_{D,\lambda_t,t}. \quad (46)$$

Furthermore, (36) and (37) yield

$$\left\| (L_{K,t} + \lambda_t I)^{1/2} (L_{K,D,t} + \lambda_t I)^{-1} (L_{K,D,t} - L_{K,t}) (Q_t^* - Q_{D,\lambda_t,t}^*) \right\|_{K,t} \leq \mathcal{A}_{D,\lambda_t,t} \mathcal{U}_{D,\lambda_t,t, Q_t^* - Q_{D,\lambda_t,t}^*}. \quad (47)$$

To bound the last term in (45), we notice

$$\left\| (L_{K,t} + \lambda_t I)^{1/2} (L_{K,D,t} + \lambda_t I)^{-1} L_{K,t} (Q_t^* - Q_{D,\lambda_t,t}^*) \right\|_{K,t} \leq \mathcal{A}_{D,\lambda_t,t} \|Q_t^* - Q_{D,\lambda_t,t}^*\|_{\mathcal{L}_t^2}.$$

But Assumption 2, (4), (17), and (29) show

$$\begin{aligned} \|Q_t^* - Q_{D,\lambda_t,t}^*\|_{\mathcal{L}_t^2}^2 &= E \left[(Q_{D,\lambda_t,t}^*(X_t) - Q_t^*(X_t))^2 \middle| D \right] \\ &= E \left[\left(\max_{a_{t+1}} Q_{D,\lambda_{t+1},t+1}(S_{1:t+1}, A_{1:t}, a_{t+1}) - \max_{a_{t+1}} Q_{t+1}^*(S_{1:t+1}, A_{1:t}, a_{t+1}) \right)^2 \middle| D \right] \\ &\leq E \left[\max_{a_{t+1}} (Q_{D,\lambda_{t+1},t+1}(S_{1:t+1}, A_{1:t}, a_{t+1}) - Q_{t+1}^*(S_{1:t+1}, A_{1:t}, a_{t+1}))^2 \middle| D \right] \\ &\leq E \left[\mu \sum_{a \in \mathcal{A}_{t+1}} (Q_{D,\lambda_{t+1},t+1}(S_{1:t+1}, A_{1:t}, a) - Q_{t+1}^*(S_{1:t+1}, A_{1:t}, a))^2 p_t(a|S_{1:t+1}, A_{1:t}) \middle| D \right] \\ &= \mu E \left[(Q_{D,\lambda_{t+1},t+1} - Q_{t+1}^*)^2 \middle| D \right] = \mu \|Q_{D,\lambda_{t+1},t+1} - Q_{t+1}^*\|_{\mathcal{L}_{t+1}^2}^2. \end{aligned}$$

Therefore,

$$\left\| (L_{K,t} + \lambda_t I)^{1/2} (L_{K,D,t} + \lambda_t I)^{-1} L_{K,t} (Q_t^* - Q_{D,\lambda_t,t}^*) \right\|_{K,t} \leq \mu^{1/2} \mathcal{A}_{D,\lambda_t,t} \|Q_{D,\lambda_{t+1},t+1} - Q_{t+1}^*\|_{\mathcal{L}_{t+1}^2}. \quad (48)$$

Plugging (46), (47), (48) into (45), we obtain (44) directly. This finishes the proof of Lemma 3. \square

Using Proposition 1, Lemma 1, Lemma 2 and Lemma 3, we can derive the following oracle inequality for KRR-DTR.

PROPOSITION 2. *Under Assumption 2 and Assumption 3 with $\frac{1}{2} \leq r \leq 1$, we have*

$$\begin{aligned} &\left\| (L_{K,t} + \lambda_t I)^{1/2} (Q_{D,\lambda_t,t} - Q_t^*) \right\|_{K,t} \\ &\leq \sum_{\ell=t}^T \left(\mu^{\frac{1}{2}} \mathcal{A}_{D,\lambda_\ell,\ell} \right)^{\ell-t} \mathcal{A}_{D,\lambda_\ell,\ell} \left(\lambda_t^r \|h_t\|_{\mathcal{L}_t^2} + \mathcal{P}_{D,\lambda_\ell,\ell} + \mathcal{S}_{D,\lambda_\ell,\ell} + \mathcal{U}_{D,\lambda_\ell,\ell,Q_\ell^* - Q_{D,\lambda_\ell,\ell}^*} \right). \end{aligned}$$

Proof. Inserting (42), (43) and (44) into (41), we obtain for any $t = 1, 2, \dots, T$,

$$\begin{aligned} &\left\| (L_{K,t} + \lambda_t I)^{1/2} (Q_{D,\lambda_t,t} - Q_t^*) \right\|_{K,t} \\ &\leq \mathcal{A}_{D,\lambda_t,t} \left(\lambda_t^r \|h_t\|_{\mathcal{L}_t^2} + \mathcal{P}_{D,\lambda_t,t} + \mathcal{S}_{D,\lambda_t,t} + \mathcal{U}_{D,\lambda_t,t,Q_t^* - Q_{D,\lambda_t,t}^*} \right) + \mu^{\frac{1}{2}} \mathcal{A}_{D,\lambda_t,t} \|Q_{D,\lambda_{t+1},t+1} - Q_{t+1}^*\|_{\mathcal{L}_{t+1}^2}. \end{aligned}$$

It then follows from $Q_{D,\lambda_{T+1},T+1} = Q_{T+1}^* = 0$ that

$$\begin{aligned} &\left\| (L_{K,t} + \lambda_t I)^{1/2} (Q_{D,\lambda_t,t} - Q_t^*) \right\|_{K,t} \\ &\leq \sum_{\ell=t}^T \left(\mu^{\frac{1}{2}} \mathcal{A}_{D,\lambda_\ell,\ell} \right)^{\ell-t} \mathcal{A}_{D,\lambda_\ell,\ell} \left(\lambda_t^r \|h_t\|_{\mathcal{L}_t^2} + \mathcal{P}_{D,\lambda_\ell,\ell} + \mathcal{S}_{D,\lambda_\ell,\ell} + \mathcal{U}_{D,\lambda_\ell,\ell,Q_\ell^* - Q_{D,\lambda_\ell,\ell}^*} \right). \end{aligned}$$

The proof of Proposition 2 is completed. \square

D.3. Error decomposition for DKRR-DTR

The generalization error of DKRR-DTR also requires the following error decomposition.

PROPOSITION 3. *For any $1 \leq t \leq T$, it holds that*

$$\begin{aligned} & \| (L_{K,t} + \lambda_t I)^{1/2} (\bar{Q}_{D,\lambda_t,t} - Q_t^*) \|_{K,t} \\ & \leq \sum_{j=1}^m \frac{|D_j|}{|D|} \mathcal{W}_{D_j,\lambda_t,t} \| (L_{K,t} + \lambda_t I)^{1/2} (Q_{D_j,\lambda_t,t} - Q_t^*) \|_{K,t} + \mathcal{U}_{D,\lambda_t,t,Q_t^*} + \| Q_{D,\lambda_t,t}^\oplus - Q_t^* \|_{\mathcal{L}_t^2}. \end{aligned}$$

Proof. Similar to (28), it follows from (13) and (14) that

$$\bar{Q}_{D,\lambda_t,t} = \sum_{j=1}^m \frac{|D_j|}{|D|} (L_{K,D_j,t} + \lambda_t I)^{-1} S_{D_j,t}^T \bar{\mathbf{y}}_{j,t},$$

where $\bar{\mathbf{y}}_{j,t} := (\bar{y}_{1,j,t}, \dots, \bar{y}_{|D_j|,j,t})^T$. Then

$$\begin{aligned} \| (L_{K,t} + \lambda_t I)^{1/2} (\bar{Q}_{D,\lambda_t,t} - Q_t^*) \|_{K,t} & \leq \left\| (L_{K,t} + \lambda_t I)^{1/2} \left(\sum_{j=1}^m \frac{|D_j|}{|D|} (L_{K,t} + \lambda_t I)^{-1} S_{D_j,t}^T \bar{\mathbf{y}}_{j,t} - Q_t^* \right) \right\|_{K,t} \\ & + \left\| (L_{K,t} + \lambda_t I)^{1/2} \sum_{j=1}^m \frac{|D_j|}{|D|} ((L_{K,D_j,t} + \lambda_t I)^{-1} - (L_{K,t} + \lambda_t I)^{-1}) S_{D_j,t}^T \bar{\mathbf{y}}_{j,t} \right\|_{K,t}. \end{aligned}$$

But

$$\begin{aligned} & ((L_{K,D_j,t} + \lambda_t I)^{-1} - (L_{K,t} + \lambda_t I)^{-1}) S_{D_j,t}^T \bar{\mathbf{y}}_{j,t} = (L_{K,t} + \lambda_t I)^{-1} (L_{K,t} - L_{K,D_j,t}) Q_{D_j,\lambda_t,t} \\ & = (L_{K,t} + \lambda_t I)^{-1} (L_{K,t} - L_{K,D_j,t}) (Q_{D_j,\lambda_t,t} - Q_t^*) + (L_{K,t} + \lambda_t I)^{-1} (L_{K,t} - L_{K,D_j,t}) Q_t^*, \\ & \sum_{j=1}^m \frac{|D_j|}{|D|} (L_{K,t} + \lambda_t I)^{-1} S_{D_j,t}^T \bar{\mathbf{y}}_{j,t} = (L_{K,t} + \lambda_t I)^{-1} S_{D,t}^T \bar{\mathbf{y}}_t, \end{aligned}$$

and

$$\sum_{j=1}^m \frac{|D_j|}{|D|} (L_{K,t} + \lambda_t I)^{-1} (L_{K,t} - L_{K,D_j,t}) Q_t^* = (L_{K,t} + \lambda_t I)^{-1} (L_{K,t} - L_{K,D,t}) Q_t^*.$$

Therefore, Jensen's inequality together with (31) yields

$$\begin{aligned} & \| (L_{K,t} + \lambda_t I)^{1/2} (\bar{Q}_{D,\lambda_t,t} - Q_t^*) \|_{K,t} \leq \left\| \sum_{j=1}^m \frac{|D_j|}{|D|} (L_{K,t} + \lambda_t I)^{-1/2} (L_{K,t} - L_{K,D_j,t}) (Q_{D_j,\lambda_t,t} - Q_t^*) \right\|_{K,t} \\ & + \| (L_{K,t} + \lambda_t I)^{-1/2} (L_{K,t} - L_{K,D,t}) Q_t^* \|_{K,t} + \| (L_{K,t} + \lambda_t I)^{1/2} (Q_{D,\lambda_t,t}^\oplus - Q_t^*) \|_{K,t} \\ & \leq \sum_{j=1}^m \frac{|D_j|}{|D|} \mathcal{W}_{D_j,\lambda_t,t} \| (L_{K,t} + \lambda_t I)^{1/2} (Q_{D_j,\lambda_t,t} - Q_t^*) \|_{K,t} + \mathcal{U}_{D,\lambda_t,t,Q_t^*} \\ & + \| (L_{K,t} + \lambda_t I)^{1/2} (Q_{D,\lambda_t,t}^\oplus - Q_t^*) \|_{K,t}. \end{aligned}$$

This completes the proof of Proposition 3. \square

Our following lemma presents an upper bound of $\| (L_{K,t} + \lambda_t I)^{1/2} (Q_{D,\lambda_t,t}^\oplus - Q_t^*) \|_{K,t}$.

LEMMA 4. Under Assumption 2 and Assumption 3 with $\frac{1}{2} \leq r \leq 1$, for $\forall t = 1, \dots, T$, there holds

$$\begin{aligned} \|(L_{K,t} + \lambda_t I)^{1/2}(Q_{D,\lambda_t,t}^\oplus - Q_t^*)\|_{K,t} &\leq \mathcal{A}_{D,\lambda_t,t} \left(\lambda_t^r \|h_t\|_{\mathcal{L}_t^2} + \mathcal{P}_{D,\lambda_t,t} + \bar{\mathcal{S}}_{D,\lambda_t,t} + \mathcal{U}_{D,\lambda_t,t,Q_t^* - \bar{Q}_{D,\lambda_t,t}^*} \right) \\ &\quad + \mu^{1/2} \mathcal{A}_{D,\lambda_t,t} \|\bar{Q}_{D,\lambda_{t+1},t+1} - Q_{t+1}^*\|_{\mathcal{L}_{t+1}^2}. \end{aligned}$$

Proof. The proof of the lemma is almost the same as that in bounding $\|(L_{K,t} + \lambda_t I)^{1/2}(Q_{D,\lambda_t,t} - Q_t^*)\|_{K,t}$ in the previous subsection. For the sake of completeness, we sketch the proof. Due to the triangle inequality, it holds that

$$\begin{aligned} \|(L_{K,t} + \lambda_t I)^{1/2}(Q_{D,\lambda_t,t}^\oplus - Q_t^*)\|_{K,t} &\leq \|(L_{K,t} + \lambda_t I)^{1/2}(Q_{D,\lambda_t,t}^\diamond - Q_t^*)\|_{K,t} \\ &\quad + \|(L_{K,t} + \lambda_t I)^{1/2}(Q_{D,\lambda_t,t}^\diamond - \hat{Q}_{D,\lambda_t,t})\|_{K,t} + \|(L_{K,t} + \lambda_t I)^{1/2}(Q_{D,\lambda_t,t}^\oplus - \hat{Q}_{D,\lambda_t,t})\|_{K,t}. \end{aligned}$$

Then, it follows from Lemma 1 and Lemma 2 that

$$\begin{aligned} \|(L_{K,t} + \lambda_t I)^{1/2}(Q_{D,\lambda_t,t}^\oplus - Q_t^*)\|_{K,t} &\leq \lambda_t^r \mathcal{A}_{D,\lambda_t,t} \|h_t\|_{\mathcal{L}_t^2} + \mathcal{A}_{D,\lambda_t,t} \mathcal{P}_{D,\lambda_t,t} \\ &\quad + \|(L_{K,t} + \lambda_t I)^{1/2}(Q_{D,\lambda_t,t}^\oplus - \hat{Q}_{D,\lambda_t,t})\|_{K,t}. \end{aligned}$$

Similar as the approach in proving Lemma 3, we obtain from (29) and (31) that

$$\begin{aligned} \|(L_{K,t} + \lambda_t I)^{1/2}(Q_{D,\lambda_t,t}^\oplus - \hat{Q}_{D,\lambda_t,t})\|_{K,t} &\leq \|(L_{K,t} + \lambda_t I)^{1/2} (L_{K,D,t} + \lambda_t I)^{-1} L_{K,t}(Q_t^* - \bar{Q}_{D,\lambda_t,t}^*)\|_{K,t} \\ &\quad + \|(L_{K,t} + \lambda_t I)^{1/2} (L_{K,D,t} + \lambda_t I)^{-1} (L_{K,D,t} - L_{K,t})(Q_t^* - \bar{Q}_{D,\lambda_t,t}^*)\|_{K,t} \\ &\quad + \|(L_{K,t} + \lambda_t I)^{1/2} (L_{K,D,t} + \lambda_t I)^{-1} (S_{D,t}^T(\mathbf{y}_{D,t}^* - \bar{\mathbf{y}}_{D,t}) - L_{K,D,t}(Q_t^* - \bar{Q}_{D,\lambda_t,t}^*))\|_{K,t} \\ &\leq \mathcal{A}_{D,\lambda_t,t} \bar{\mathcal{S}}_{D,\lambda_t,t} + \mathcal{A}_{D,\lambda_t,t} \mathcal{U}_{D,\lambda_t,t,Q_t^* - \bar{Q}_{D,\lambda_t,t}^*} + \mu^{1/2} \mathcal{A}_{D,\lambda_t,t} \|\bar{Q}_{D,\lambda_{t+1},t+1} - Q_{t+1}^*\|_{\mathcal{L}_{t+1}^2}. \end{aligned}$$

Therefore,

$$\begin{aligned} \|(L_{K,t} + \lambda_t I)^{1/2}(Q_{D,\lambda_t,t}^\oplus - Q_t^*)\|_{K,t} &\leq \mathcal{A}_{D,\lambda_t,t} \left(\lambda_t^r \|h_t\|_{\mathcal{L}_t^2} + \mathcal{P}_{D,\lambda_t,t} + \bar{\mathcal{S}}_{D,\lambda_t,t} + \mathcal{U}_{D,\lambda_t,t,Q_t^* - \bar{Q}_{D,\lambda_t,t}^*} \right) \\ &\quad + \mu^{1/2} \mathcal{A}_{D,\lambda_t,t} \|\bar{Q}_{D,\lambda_{t+1},t+1} - Q_{t+1}^*\|_{\mathcal{L}_{t+1}^2}. \end{aligned}$$

This completes the proof of Lemma 4. \square

We also bound $\|(L_{K,t} + \lambda_t I)^{1/2}(Q_{D,j,\lambda_t,t} - Q_t^*)\|_{K,t}$ in the following lemma.

LEMMA 5. Under Assumption 2 and Assumption 3 with $\frac{1}{2} \leq r \leq 1$, for $\forall t = 1, \dots, T$, there holds

$$\begin{aligned} \|(L_{K,t} + \lambda_t I)^{1/2}(Q_{D,j,\lambda_t,t} - Q_t^*)\|_{K,t} &\leq \mathcal{A}_{D,j,\lambda_t,t} \left(\lambda_t^r \|h_t\|_{\mathcal{L}_t^2} + \mathcal{P}_{D,j,\lambda_t,t} + \bar{\mathcal{S}}_{D,j,\lambda_t,t} + \mathcal{U}_{D,j,\lambda_t,t,Q_t^* - \bar{Q}_{D,j,\lambda_t,t}^*} \right) \\ &\quad + \mu^{1/2} \mathcal{A}_{D,j,\lambda_t,t} \|\bar{Q}_{D,\lambda_{t+1},t+1} - Q_{t+1}^*\|_{\mathcal{L}_{t+1}^2}. \end{aligned}$$

Proof. It follows from Lemma 1 and Lemma 2 with $D = D_j$ that

$$\begin{aligned} & \left\| (L_{K,t} + \lambda_t I)^{1/2} (Q_{D_j, \lambda_t, t} - Q_t^*) \right\|_{K,t} \leq \left\| (L_{K,t} + \lambda_t I)^{1/2} \left(Q_{D_j, \lambda_t, t}^* - Q_t^* \right) \right\|_{K,t} \\ & + \left\| (L_{K,t} + \lambda_t I)^{1/2} \left(Q_{D_j, \lambda_t, t}^* - \hat{Q}_{D_j, \lambda_t, t} \right) \right\|_{K,t} + \left\| (L_{K,t} + \lambda_t I)^{1/2} (Q_{D_j, \lambda_t, t} - \hat{Q}_{D_j, \lambda_t, t}) \right\|_{K,t} \\ & \leq \lambda_t^r \mathcal{A}_{D_j, \lambda_t, t} \|h_t\|_{\mathcal{L}_t^2} + \mathcal{A}_{D_j, \lambda_t, t} \mathcal{P}_{D_j, \lambda_t, t} + \left\| (L_{K,t} + \lambda_t I)^{1/2} (Q_{D_j, \lambda_t, t} - \hat{Q}_{D_j, \lambda_t, t}) \right\|_{K,t}. \end{aligned}$$

But for any $t = 1, \dots, T$, we have from (13), (30), and the same method in proving Lemma 3 that

$$\begin{aligned} & \left\| (L_{K,t} + \lambda_t I)^{1/2} (Q_{D_j, \lambda_t, t} - \hat{Q}_{D_j, \lambda_t, t}) \right\|_{K,t} \leq \left\| (L_{K,t} + \lambda_t I)^{1/2} (L_{K, D_j, t} + \lambda_t I)^{-1} L_{K,t} (Q_t^* - \bar{Q}_{D_j, \lambda_t, t}^*) \right\|_{K,t} \\ & + \left\| (L_{K,t} + \lambda_t I)^{1/2} (L_{K, D_j, t} + \lambda_t I)^{-1} \left(S_{D_j, t}^T (\mathbf{y}_{D_j, t}^* - \bar{\mathbf{y}}_{D_j, t}) - L_{K, D, t} (Q_t^* - \bar{Q}_{D_j, \lambda_t, t}^*) \right) \right\|_{K,t} \\ & + \left\| (L_{K,t} + \lambda_t I)^{1/2} (L_{K, D_j, t} + \lambda_t I)^{-1} (L_{K, D_j, t} - L_{K,t}) (Q_t^* - \bar{Q}_{D_j, \lambda_t, t}^*) \right\|_{K,t} \\ & \leq \mathcal{A}_{D_j, \lambda_t, t} \bar{\mathcal{S}}_{D_j, \lambda_t, t} + \mathcal{A}_{D_j, \lambda_t, t} \mathcal{U}_{D_j, \lambda_t, t, Q_t^* - \bar{Q}_{D_j, \lambda_t, t}^*} + \mu^{1/2} \mathcal{A}_{D_j, \lambda_t, t} \left\| \bar{Q}_{D, \lambda_{t+1}, t+1} - Q_{t+1}^* \right\|_{\mathcal{L}_{t+1}^2}. \end{aligned}$$

Therefore,

$$\begin{aligned} & \left\| (L_{K,t} + \lambda_t I)^{1/2} (Q_{D_j, \lambda_t, t} - Q_t^*) \right\|_{K,t} \leq \mathcal{A}_{D_j, \lambda_t, t} \left(\lambda_t^r \|h_t\|_{\mathcal{L}_t^2} + \mathcal{P}_{D_j, \lambda_t, t} + \bar{\mathcal{S}}_{D_j, \lambda_t, t} + \mathcal{U}_{D_j, \lambda_t, t, Q_t^* - \bar{Q}_{D_j, \lambda_t, t}^*} \right) \\ & + \mu^{-1/2} \mathcal{A}_{D_j, \lambda_t, t} \left\| \bar{Q}_{D, \lambda_{t+1}, t+1} - Q_{t+1}^* \right\|_{\mathcal{L}_{t+1}^2}. \end{aligned}$$

This completes the proof of Lemma 5. \square

Based on Lemma 4, Lemma 5, and Proposition 3, we can derive the following oracle inequality.

PROPOSITION 4. *Under Assumption 2 and Assumption 3 with $\frac{1}{2} \leq r \leq 1$, it holds that*

$$\begin{aligned} & \left\| (L_{K,t} + \lambda_t I)^{1/2} (\bar{Q}_{D, \lambda_t, t} - Q_t^*) \right\|_{K,t} \\ & \leq \sum_{\ell=t}^T \prod_{k=t+1}^{\ell} \left(\left(\sum_{j=1}^m \frac{|D_j|}{|D|} \mathcal{W}_{D_j, \lambda_k, k} \mathcal{A}_{D_j, \lambda_k, k} + \mathcal{A}_{D, \lambda_k, k} \right) \mu^{1/2} \right) \\ & \times \left(\sum_{j=1}^m \frac{|D_j|}{|D|} \mathcal{W}_{D_j, \lambda_{\ell}, \ell} \mathcal{A}_{D_j, \lambda_{\ell}, \ell} \left(\lambda_{\ell}^r \|h_{\ell}\|_{\mathcal{L}_{\ell}^2} + \mathcal{P}_{D_j, \lambda_{\ell}, \ell} + \bar{\mathcal{S}}_{D_j, \lambda_{\ell}, \ell} + \mathcal{U}_{D_j, \lambda_{\ell}, \ell, Q_{\ell}^* - \bar{Q}_{D_j, \lambda_{\ell}, \ell}^*} \right) \right. \\ & \left. + \mathcal{A}_{D, \lambda_{\ell}, \ell} \left(\lambda_{\ell}^r \|h_{\ell}\|_{\mathcal{L}_{\ell}^2} + \mathcal{P}_{D, \lambda_{\ell}, \ell} + \bar{\mathcal{S}}_{D, \lambda_{\ell}, \ell} + \mathcal{U}_{D, \lambda_{\ell}, \ell, Q_{\ell}^* - \bar{Q}_{D, \lambda_{\ell}, \ell}^*} \right) + \mathcal{U}_{D, \lambda_{\ell}, \ell, Q_{\ell}^*} \right). \end{aligned}$$

Proof. Inserting Lemma 4 and Lemma 5 into Proposition 3, we obtain

$$\begin{aligned} & \left\| (L_{K,t} + \lambda_t I)^{1/2} (\bar{Q}_{D, \lambda_t, t} - Q_t^*) \right\|_{K,t} \\ & \leq \sum_{j=1}^m \frac{|D_j|}{|D|} \mathcal{W}_{D_j, \lambda_t, t} \mathcal{A}_{D_j, \lambda_t, t} \left(\lambda_t^r \|h_t\|_{\mathcal{L}_t^2} + \mathcal{P}_{D_j, \lambda_t, t} + \bar{\mathcal{S}}_{D_j, \lambda_t, t} + \mathcal{U}_{D_j, \lambda_t, t, Q_t^* - \bar{Q}_{D_j, \lambda_t, t}^*} \right) \\ & + \mathcal{A}_{D, \lambda_t, t} \left(\lambda_t^r \|h_t\|_{\mathcal{L}_t^2} + \mathcal{P}_{D, \lambda_t, t} + \bar{\mathcal{S}}_{D, \lambda_t, t} + \mathcal{U}_{D, \lambda_t, t, Q_t^* - \bar{Q}_{D, \lambda_t, t}^*} \right) + \mathcal{U}_{D, \lambda_t, t, Q_t^*} \end{aligned}$$

$$\begin{aligned}
& + \left(\sum_{j=1}^m \frac{|D_j|}{|D|} \mathcal{W}_{D_j, \lambda_t, t} \mathcal{A}_{D_j, \lambda_t, t} + \mathcal{A}_{D, \lambda_t, t} \right) \mu^{1/2} \left\| \overline{Q}_{D, \lambda_{t+1}, t+1} - Q_{t+1}^* \right\|_{\mathcal{L}_{t+1}^2} \\
& \leq \sum_{\ell=t}^T \prod_{k=t+1}^{\ell} \left(\left(\sum_{j=1}^m \frac{|D_j|}{|D|} \mathcal{W}_{D_j, \lambda_k, k} \mathcal{A}_{D_j, \lambda_k, k} + \mathcal{A}_{D, \lambda_k, k} \right) \mu^{1/2} \right) \\
& \quad \times \left(\sum_{j=1}^m \frac{|D_j|}{|D|} \mathcal{W}_{D_j, \lambda_{\ell}, \ell} \mathcal{A}_{D_j, \lambda_{\ell}, \ell} \left(\lambda_{\ell}^r \|h_{\ell}\|_{\mathcal{L}_{\ell}^2} + \mathcal{P}_{D_j, \lambda_{\ell}, \ell} + \overline{\mathcal{S}}_{D_j, \lambda_{\ell}, \ell} + \mathcal{U}_{D_j, \lambda_{\ell}, \ell, Q_{\ell}^* - \overline{Q}_{D_j, \lambda_{\ell}, \ell}^*} \right) \right. \\
& \quad \left. + \mathcal{A}_{D, \lambda_{\ell}, \ell} \left(\lambda_{\ell}^r \|h_{\ell}\|_{\mathcal{L}_{\ell}^2} + \mathcal{P}_{D, \lambda_{\ell}, \ell} + \overline{\mathcal{S}}_{D, \lambda_{\ell}, \ell} + \mathcal{U}_{D, \lambda_{\ell}, \ell, Q_{\ell}^* - \overline{Q}_{D, \lambda_{\ell}, \ell}^*} \right) + \mathcal{U}_{D, \lambda_{\ell}, \ell, Q_{\ell}^*} \right).
\end{aligned}$$

This completes the proof of Proposition 4. \square

D.4. Bounds of operator differences

In this part, we aim at bounding the operator differences. The first lemma focuses on bounding $\mathcal{W}_{D, \lambda_t, t}$, which can be found in (Lin et al. 2020, Lemma 6).

LEMMA 6. *Let $0 < \delta \leq 1$. If Assumption 1 holds and $0 < \lambda \leq 1$, then with confidence $1 - \delta$, it holds that*

$$\mathcal{W}_{D, \lambda_t, t} \leq C_1^* \mathcal{B}_{D, \lambda_t, t} \log \frac{4}{\delta}, \quad t = 1, \dots, T,$$

where $C_1^* := \max\{(\kappa^2 + 1)/3, 2\sqrt{\kappa^2 + 1}\}$ and

$$\mathcal{B}_{D, \lambda_t, t} := \frac{1 + \log(1 + \mathcal{N}_t(\lambda_t))}{\lambda |D|} + \sqrt{\frac{1 + \log(1 + \mathcal{N}_t(\lambda_t))}{\lambda |D|}}. \quad (49)$$

The second one aims at bounding $\mathcal{A}_{D, \lambda_t, t}$, which can be found in (Lin et al. 2020, Lemma 7).

LEMMA 7. *If Assumption 1 holds and $0 < \lambda \leq 1$, then for $\delta \geq 4 \exp\{-1/(2C_1^* \mathcal{B}_{D, \lambda_t, t})\}$, with confidence $1 - \delta$, it holds that $\mathcal{A}_{D, \lambda_t, t} \leq 2$ for $t = 1, \dots, T$.*

The bound of $\mathcal{U}_{D, \lambda_t, t, f}$, provided in (Lin et al. 2017, Lemma 18), is shown in the following lemma.

LEMMA 8. *Under Assumption 1, for any $0 < \delta < 1$ and $\|f\|_{L^\infty} < \infty$, with confidence at least $1 - \delta$, it holds that*

$$\mathcal{U}_{D, \lambda_t, t, f} \leq \frac{2\|f\|_{L^\infty} \log(2/\delta)}{\sqrt{|D|}} \left\{ \frac{\kappa}{\sqrt{|D|\lambda_t}} + \sqrt{\mathcal{N}(\lambda_t)} \right\}, \quad t = 1, \dots, T.$$

To bound $\mathcal{P}_{D, \lambda_t, t}$, $\mathcal{S}_{D, \lambda_t, t}$ and $\overline{\mathcal{S}}_{D, \lambda_t, t}$, we should introduce a Hilbert valued Bernstein inequality established in (Pinelis 1994).

LEMMA 9. *For a random variable ξ on (\mathcal{Z}, ρ) with values in a separable Hilbert space $(H, \|\cdot\|)$ satisfying $\|\xi\| \leq \bar{M} < \infty$ almost surely, and a random sample $\{z_i\}_{i=1}^s$ independent drawn according to ρ , there holds with confidence $1 - \tilde{\delta}$ that*

$$\left\| \frac{1}{s} \sum_{i=1}^s (\xi(z_i) - E[\xi]) \right\| \leq \frac{2\bar{M} \log(2/\tilde{\delta})}{s} + \sqrt{\frac{2E[\|\xi\|^2] \log(2/\tilde{\delta})}{s}}.$$

With the help of Lemma 9, we can derive the following concentration inequality, which is crucial to bound $\mathcal{P}_{D,\lambda_t,t}$, $\mathcal{S}_{D,\lambda_t,t}$ and $\bar{\mathcal{S}}_{D,\lambda_t,t}$.

LEMMA 10. *Let $0 < \delta < 1$, $\mathbf{y}_D = (y_1, \dots, y_{|D|})^T \in \mathbb{R}^{|D|}$ with $|y_i| \leq \tilde{M}$ almost surely, and $g(x_i) = E[Y_i|x_i]$.*

Under Assumption 1, with confidence $1 - \delta$, it holds that

$$\|(L_{K,t} + \lambda_t I)^{-1/2}(S_{D,t}^T \mathbf{y}_D - L_{K,D}g)\|_{K,t} \leq \frac{2\sqrt{2}\tilde{M}\log(2/\delta)}{\sqrt{|D|}} \left(\frac{\sqrt{2}}{\sqrt{|D|\lambda_t}} + \sqrt{\mathcal{N}_t(\lambda_t)} \right).$$

Proof. Denote $z_i = (x_i, y_i)$ and $\eta_t(z_i) = (L_{K,t} + \lambda_t I)^{-1/2}(y_i - g(x_i))K_{x_i} \in \mathcal{H}_{K,t}$. Then, we have $E[\eta_t(z_i)] = 0$

and

$$\begin{aligned} \|\eta_t(z_i)\|_{K,t}^2 &= \langle (L_{K,t} + \lambda_t I)^{-1/2}(y_i - g(x_i))K_{x_i}, (L_{K,t} + \lambda_t I)^{-1/2}(y_i - g(x_i))K_{x_i} \rangle_{K,t} \\ &\leq 4\tilde{M}^2 \|(L_{K,t} + \lambda_t I)^{-1/2}(K_{x_i})\|_{K,t}^2 = 4\tilde{M}^2 \sum_{k=1}^{\infty} \frac{(\varphi_{k,t}(x_i))^2}{\sigma_{k,t} + \lambda_t}, \end{aligned}$$

where $(\sigma_{k,t}, \varphi_{k,t})_{k=1}^{\infty}$ is the normalized eigen-pairs of $L_{K,t}$. Thus, we have $\|\eta_t(z_i)\|_{K,t} \leq \frac{2\tilde{M}}{\sqrt{\lambda_t}}$ and

$$\begin{aligned} E[\|\eta_t(z_i)\|_{K,t}^2] &\leq 4\tilde{M}^2 E \left[\sum_{k=1}^{\infty} \frac{(\varphi_{k,t}(x_i))^2}{\sigma_{k,t} + \lambda_t} \right] = 4\tilde{M}^2 \sum_{k=1}^{\infty} \frac{E[\varphi_{k,t}^2(x_i)]}{\sigma_{k,t} + \lambda_t} \\ &= 4\tilde{M}^2 \sum_{k=1}^{\infty} \frac{\sigma_{k,t}}{\sigma_{k,t} + \lambda_t} = 4\tilde{M}^2 \text{Tr}(L_{K,t}(L_{K,t} + \lambda_t I)^{-1}) = 4\tilde{M}^2 \mathcal{N}_t(\lambda_t), \end{aligned}$$

where we used the fact $E[\varphi_{k,t}^2] = \sigma_{k,t}$ which was proven in (Lin et al. 2017, eqs.(51)). Therefore, it follows from Lemma 9 that with confidence $1 - \delta$, it holds that

$$\left\| \frac{1}{|D|} \sum_{i=1}^{|D|} \eta_t(z_i) \right\| \leq \frac{4\tilde{M}\log(2/\delta)}{\sqrt{\lambda_t}|D|} + \sqrt{\frac{8\tilde{M}^2\mathcal{N}_t(\lambda_t)\log(2/\delta)}{|D|}}.$$

This completes the proof of Lemma 10. \square

Setting $y_i = y_{i,t}^*$ and $\tilde{M} = (T-t+1)M$ in Lemma 10, we can derive the following bound of $\mathcal{P}_{D,\lambda_t,t}$.

LEMMA 11. *Let $0 < \delta < 1$. Under Assumption 1, with confidence $1 - \delta$, it holds that*

$$\mathcal{P}_{D,\lambda_t,t} \leq \frac{2\sqrt{2}(T-t+1)M\log(2/\delta)}{\sqrt{|D|}} \left(\frac{\sqrt{2}}{\sqrt{|D|\lambda_t}} + \sqrt{\mathcal{N}_t(\lambda_t)} \right).$$

Unlike $\mathcal{P}_{D,\lambda_t,t}$, the bounds of $\mathcal{S}_{D,\lambda_t,t}$ and $\bar{\mathcal{S}}_{D,\lambda_t,t}$ are much more sophisticated, which requires an upper bound of $\|Q_{D,\lambda_t,t}\|_{\mathcal{L}_t^{\infty}}$ and $\|\bar{Q}_{D,\lambda_t,t}\|_{\mathcal{L}_t^{\infty}}$ for $\forall t = 1, \dots, T$. We leave them in the next subsection.

D.5. Uniform bounds of \mathbf{Q} -functions

In this part, we aim at deriving $\|Q_{D,\lambda_t,t}\|_{\mathcal{L}_t^\infty}$ and $\|\bar{Q}_{D,\lambda_t,t}\|_{\mathcal{L}_t^\infty}$ so that $y_{i,t}$ and $\bar{y}_{i,t}$ can also be uniformly bounded. The following lemma presents an iterative relation between $\|Q_{D,\lambda_{t+1},t+1}\|_{\mathcal{L}_{t+1}^\infty}$ and $\|Q_{D,\lambda_t,t}\|_{\mathcal{L}_t^\infty}$.

LEMMA 12. *Let $0 \leq \delta \leq 1$ satisfy*

$$\delta \geq 8T \exp \left\{ -\frac{2r+s}{4sC_1^*(\log(C_0+1)+2)} |D|^{\frac{2r+s-1}{8r+4s}} \log^{-1} |D| \right\}. \quad (50)$$

Under Assumptions 1-4 with $\frac{1}{2} \leq r \leq 1$ and $0 < s \leq 1$, if $\lambda_t = |D|^{-\frac{1}{2r+s}}$ for $t = 1, \dots, T$, then with confidence $1 - \delta/T$, it holds that

$$\|Q_{D,\lambda_t,t}\|_{\mathcal{L}_t^\infty} + M \leq \bar{C} \sum_{\ell=t}^T (T-\ell+2) (2\mu^{1/2})^{\ell-t} \left(\|Q_{D,\lambda_{\ell+1},\ell+1}\|_{\mathcal{L}_{\ell+1}^\infty} + M \right), \quad t = 1, 2, \dots, T, \quad (51)$$

where \bar{C} is a constant depending only on C_0 , κ , r , s , and $\max_{t=1,\dots,T} \|h_t\|_{\mathcal{L}_t^2}$.

Proof. Denote $\Phi_t = \|Q_{D,\lambda_t,t}\|_{\mathcal{L}_t^\infty}$. Since $\lambda_1 = \dots = \lambda_T = |D|^{-\frac{1}{2r+s}}$, we have from Assumption 4 that $\mathcal{N}_t(\lambda_t) \leq C_0 \lambda_t^{-s} = C_0 |D|^{\frac{s}{2r+s}}$ for $\forall t = 1, 2, \dots, T$. Then

$$\frac{1}{\sqrt{|D|}} \left(\frac{1}{\sqrt{|D|\lambda_t}} + \sqrt{\mathcal{N}_t(\lambda_t)} \right) \leq (\sqrt{C_0} + 1) |D|^{\frac{-r}{2r+s}}, \quad \forall t = 1, 2, \dots, T, \quad (52)$$

and

$$\mathcal{B}_{D,\lambda_t,t} \leq \frac{2s}{2r+s} (\log(C_0+1)+2) |D|^{\frac{1-2r-s}{4r+2s}} \log |D|. \quad (53)$$

Therefore, Lemma 7 and Lemma 11 yield that, with confidence $1 - \delta/(4T)$ with δ satisfying (50), there hold for any $t = 1, \dots, T$,

$$\mathcal{A}_{D,\lambda_t,t} \leq 2, \quad (54)$$

$$\mathcal{P}_{D,\lambda_t,t} \leq 4(T-t+1)M(\sqrt{C_0}+1)|D|^{\frac{-r}{2r+s}} \log \frac{8T}{\delta}. \quad (55)$$

We get from Assumption 1 that $|y_{i,t}| \leq M + \Phi_{t+1}$ almost surely. Hence, it follows from (16), Lemma 8 with $f = Q_t^* - Q_{D,\lambda_t,t}^*$, and Lemma 10 with $y_i = y_{i,t} - y_{i,t}^*$ and $\tilde{M} = (T-t+2)M + \Phi_{t+1}$ that

$$\mathcal{U}_{D,\lambda_t,t,Q_t^*-Q_{D,\lambda_t,t}^*} \leq 2((T-t+2)M + \Phi_{t+1})(\kappa+1)(\sqrt{C_0}+1)|D|^{\frac{-r}{2r+s}} \log \frac{8T}{\delta}, \quad (56)$$

$$\mathcal{S}_{D,\lambda_t,t} \leq 4((T-t+2)M + \Phi_{t+1})(\sqrt{C_0}+1)|D|^{\frac{-r}{2r+s}} \log \frac{8T}{\delta}, \quad (57)$$

hold with confidence $1 - \delta/(4T)$. Plugging (54), (55), (56), and (57) into Proposition 2, we obtain from (50) that

$$\begin{aligned} \|Q_{D,\lambda_t,t} - Q_t^*\|_{K,t} &\leq \lambda_t^{-1/2} \|(L_{K,t} + \lambda_t I)^{1/2} (Q_{D,\lambda_t,t} - Q_t^*)\|_{K,t} \\ &\leq \sum_{\ell=t}^T (T-\ell+2) (2\mu^{1/2})^{\ell-t} \left(\|h_\ell\|_{\mathcal{L}_\ell^2} + (\sqrt{C_0} + 1)(M + \Phi_{\ell+1})(2\kappa + 10) \right) |D|^{\frac{-2r+1}{4r+2s}} \log \frac{8T}{\delta} \\ &\leq \frac{(2r+s) \sum_{\ell=t}^T (T-\ell+2) (2\mu^{1/2})^{\ell-t} \left(\|h_\ell\|_{\mathcal{L}_\ell^2} + (\sqrt{C_0} + 1)(M + \Phi_{\ell+1})(2\kappa + 10) \right)}{(4sC_1^*(\log(C_0 + 1) + 2))} \\ &\leq \bar{C}_1 \sum_{\ell=t}^T (T-\ell+2) (2\mu^{1/2})^{\ell-t} (\Phi_{\ell+1} + M) \end{aligned}$$

holds with confidence $1 - \delta/T$, where δ satisfies (50), and

$$\bar{C}_1 := \frac{4(2r+s) \left(\max_{\ell=1,\dots,T} \|h_\ell\|_{\mathcal{L}_\ell^2} + (\sqrt{C_0} + 1)(2\kappa + 10) \right)}{4sC_1^*(\log(C_0 + 1) + 2)}.$$

Therefore, we have

$$\begin{aligned} \|Q_{D,\lambda_t,t}\|_{\mathcal{L}_t^\infty} + M &\leq \kappa \|Q_{D,\lambda_t,t}\|_{K,t} + M \leq \kappa \|Q_{D,\lambda_t,t} - Q_t^*\|_{K,t} + \kappa \|Q_t^*\|_{K,t} + M \\ &\leq \bar{C} \sum_{\ell=t}^T (T-\ell+2) (2\mu^{1/2})^{\ell-t} (\Phi_{\ell+1} + M), \end{aligned}$$

where $\bar{C} := \kappa \bar{C}_1 + \kappa^{2r} \max_{t=1,\dots,T} \|h_t\|_{\mathcal{L}_t^2} + 1$. This completes the proof of Lemma 12. \square

Based on the above lemma, we can derive an upper bound of $\|Q_{D,\lambda_t,t}\|_{\mathcal{L}_t^\infty}$.

PROPOSITION 5. *Let $0 \leq \delta \leq 1$ with δ satisfying (50). Under Assumptions 1-4 with $\frac{1}{2} \leq r \leq 1$ and $0 < s \leq 1$, if $\lambda_t = |D|^{-\frac{1}{2r+s}}$ for $t = 1, \dots, T$, then with confidence $1 - \delta$, it holds that*

$$\|Q_{D,\lambda_t,t}\|_{\mathcal{L}_t^\infty} \leq 2\bar{C}^T (2\mu^{1/2})^{T-t} M \prod_{\ell=t}^{T-1} \left((T-\ell+2) (2\mu^{1/2})^{\ell-t} + 1 \right) - M, \quad t = 1, \dots, T.$$

Proof. Since for any $\xi_t, \eta_t > 0$, $\xi_t \leq \sum_{\ell=t}^T \eta_\ell \xi_{\ell+1}$ implies $\xi_t \leq \prod_{\ell=t}^{T-1} (\eta_\ell + 1) \eta_T \xi_{T+1}$. Set $\xi_t = \|Q_{D,\lambda_t,t}\|_{\mathcal{L}_t^\infty} + M$ and $\eta_t = \bar{C}(T-\ell+2) (2\mu^{1/2})^{\ell-t}$. We have from (51) and $Q_{D,\lambda_{T+1},T+1} = 0$ that

$$\|Q_{D,\lambda_t,t}\|_{\mathcal{L}_t^\infty} + M \leq \prod_{\ell=t}^{T-1} \left(\bar{C}(T-\ell+2) (2\mu^{1/2})^{\ell-t} + 1 \right) 2\bar{C} (2\mu^{1/2})^{T-t} M.$$

This completes the proof Proposition 5. \square

Similar to Lemma 12, we present an iteration relation between $\|\bar{Q}_{D,\lambda_t,t}\|_{\mathcal{L}_t^\infty}$ and $\|\bar{Q}_{D,\lambda_{t+1},t+1}\|_{\mathcal{L}_{t+1}^\infty}$.

LEMMA 13. *Let $0 \leq \delta \leq 1$ satisfy*

$$\delta \geq 40Tm \exp \left\{ -\frac{2r+s}{4sC_1^*(\log(C_0 + 1) + 2)} |D|^{\frac{2r+s-1}{16r+8s}} m^{-1/2} \log^{-1} |D| \right\}. \quad (58)$$

Under Assumptions 1-4 with $\frac{1}{2} \leq r \leq 1$ and $0 < s \leq 1$, if $\lambda_t = |D|^{-\frac{1}{2r+s}}$ for $t = 1, \dots, T$, $|D_1| = \dots = |D_m|$, and m satisfies (22), then with confidence $1 - \delta/T$, it holds that

$$\|\bar{Q}_{D,\lambda_t,t}\|_{\mathcal{L}_t^\infty} + M \leq \hat{C} \sum_{\ell=t}^T (T-t+2) (2\mu^{1/2})^{\ell-t} (\Phi_{\ell+1} + M), \quad t = 1, 2, \dots, T, \quad (59)$$

where \bar{C} is a constant depending only on C_0 , κ , r , s , and $\max_{t=1,\dots,T} \|h_t\|_{\mathcal{L}_t^2}$.

Proof. Write $\Psi_t = \|\bar{Q}_{D,\lambda_t,t}\|_{\mathcal{L}_t^\infty}$. Since $|D_1| = \dots = |D_m|$ and $\lambda_1 = \dots = \lambda_T = |D|^{-\frac{1}{2r+s}}$, (22) yields

$$\frac{1}{\sqrt{|D_j|}} \left(\frac{1}{\sqrt{|D_j|\lambda_t}} + \sqrt{\mathcal{N}_t(\lambda_t)} \right) \leq (\sqrt{C_0} + 1) \sqrt{m} |D|^{\frac{-r}{2r+s}}, \quad \forall t = 1, 2, \dots, T, \quad (60)$$

and

$$\mathcal{B}_{D,\lambda_t,t} \leq \frac{2s}{2r+s} (\log(C_0 + 1) + 2) \sqrt{m} |D|^{\frac{1-2r-s}{4r+2s}} \log |D|. \quad (61)$$

From Lemma 6, Lemma 7, and Lemma 11 with $D = D_j$, we obtain that for any δ satisfying (58), with confidence $1 - \delta/(10mT)$, it holds that

$$\mathcal{W}_{D_j,\lambda_t,t} \leq C_1^* \frac{2s}{2r+s} (\log(C_0 + 1) + 2) \sqrt{m} |D|^{\frac{1-2r-s}{4r+2s}} \log |D| \log \frac{40mT}{\delta}, \quad (62)$$

$$\mathcal{A}_{D_j,\lambda_t,t} \leq 2, \quad (63)$$

$$\mathcal{P}_{D_j,\lambda_t,t} \leq 4(T-t+1)M(\sqrt{C_0} + 1) \sqrt{m} |D|^{\frac{-r}{2r+s}} \log \frac{20mT}{\delta}. \quad (64)$$

We get from Assumption 1 that $|\bar{y}_{i,t}| \leq M + \Psi_{t+1}$ almost surely. Hence, it follows from (16), Lemma 8 with $f = Q_t^* - \bar{Q}_{D,\lambda_t,t}^*$, and Lemma 10 with $y_i = \bar{y}_{i,t} - y_{i,t}^*$ and $\tilde{M} = (T-t+2)M + \Psi_{t+1}$ that

$$\mathcal{U}_{D_j,\lambda_t,t,Q_t^* - \bar{Q}_{D,\lambda_t,t}^*} \leq 2((T-t+2)M + \Psi_{t+1})(\kappa + 1)(\sqrt{C_0} + 1) \sqrt{m} |D|^{\frac{-r}{2r+s}} \log \frac{20mT}{\delta}, \quad (65)$$

$$\bar{\mathcal{S}}_{D_j,\lambda_t,t} \leq 4((T-t+2)M + \Psi_{t+1})(\sqrt{C_0} + 1) \sqrt{m} |D|^{\frac{-r}{2r+s}} \log \frac{20mT}{\delta} \quad (66)$$

hold with confidence $1 - \delta/(10mT)$. Hence, with confidence $1 - \delta/(2mT)$ with δ satisfying (58), we have from (22) that

$$\begin{aligned} & \left(\sum_{j=1}^m \frac{|D_j|}{|D|} \mathcal{W}_{D_j,\lambda_t,t} \mathcal{A}_{D_j,\lambda_t,t} + \mathcal{A}_{D,\lambda_t,t} \right)^{\ell-t} \\ & \leq \left(C_1^* \frac{2s}{2r+s} (\log(C_0 + 1) + 2) \sqrt{m} |D|^{\frac{1-2r-s}{4r+2s}} \log |D| \log \frac{40mT}{\delta} + 1 \right)^{\ell-t} \leq 2^{\ell-t} \end{aligned}$$

and

$$\begin{aligned} & \lambda_\ell^{-1/2} \sum_{j=1}^m \frac{|D_j|}{|D|} \mathcal{W}_{D_j,\lambda_\ell,t} \mathcal{A}_{D_j,\lambda_\ell,t} \left(\lambda_\ell^r \|h_\ell\|_{\mathcal{L}_\ell^2} + \mathcal{P}_{D_j,\lambda_\ell,t} + \bar{\mathcal{S}}_{D_j,\lambda_\ell,t} + \mathcal{U}_{D_j,\lambda_\ell,t,Q_\ell^* - \bar{Q}_{D_j,\lambda_\ell,t}^*} \right) \\ & \leq \hat{C}_1(T-\ell+2)(M+\Psi_{\ell+1})m|D|^{\frac{1-2r-s}{4r+2s}} \log |D| |D|^{-\frac{2r-1}{4r+2s}} \log^2 \frac{40mT}{\delta} \leq 4\hat{C}_1(T-\ell+2)(M+\Psi_{\ell+1}), \end{aligned}$$

where $\hat{C}_1 := \max_{t=1,\dots,T} \|h_t\|_{\mathcal{L}_t^2} + 4(\sqrt{C_0} + 1) + 4(\sqrt{C_0} + 1) + 2(\kappa + 1)(\sqrt{C_0} + 1)$. Similarly, we can derive from (54), (55), (56), and (57) that, with confidence $1 - \delta/(2T)$ with δ satisfying (58), it holds that

$$\begin{aligned} & \lambda_\ell^{-1/2} \mathcal{A}_{D,\lambda_\ell,\ell} \left(\lambda_\ell^r \|h_\ell\|_{\mathcal{L}_\ell^2} + \mathcal{P}_{D,\lambda_\ell,\ell} + \bar{\mathcal{S}}_{D,\lambda_\ell,\ell} + \mathcal{U}_{D,\lambda_\ell,\ell,Q_\ell^* - \bar{Q}_{D,\lambda_\ell,\ell}^*} \right) + \mathcal{U}_{D,\lambda_\ell,\ell,Q_\ell^*} \\ & \leq \hat{C}_2 (2\mu^{1/2})^{\ell-t} (\Psi_{\ell+1} + M), \end{aligned}$$

where $\hat{C}_2 := \bar{C}_1 + 1$. The above three estimates together with Proposition 4 yield that, with confidence $1 - \delta/T$, it holds that

$$\begin{aligned} & \|\bar{Q}_{D,\lambda_t,t} - Q_t^*\|_{K,t} \leq \lambda_t^{-1/2} \|(L_{K,t} + \lambda_t I)^{1/2} (\bar{Q}_{D,\lambda_t,t} - Q_t^*)\|_{K,t} \\ & \leq (\hat{C}_1 + 2\hat{C}_2) \sum_{\ell=t}^T (T - \ell + 2) (2\mu^{1/2})^{\ell-t} (\Psi_{\ell+1} + M). \end{aligned}$$

Therefore, we have

$$\begin{aligned} & \|\bar{Q}_{D,\lambda_t,t}\|_{\mathcal{L}_t^\infty} + M \leq \kappa \|\bar{Q}_{D,\lambda_t,t}\|_{K,t} + M \leq \kappa \|\bar{Q}_{D,\lambda_t,t} - Q_t^*\|_{K,t} + \kappa \|Q_t^*\|_{K,t} + M \\ & \leq \hat{C} \sum_{\ell=t}^T (T - \ell + 2) (\hat{C}_1 2\mu^{1/2})^{\ell-t} (\Psi_{\ell+1} + M), \end{aligned}$$

where $\hat{C} := \kappa(\hat{C}_1 + 2\hat{C}_2) + \kappa^{2r} \max_{t=1,\dots,T} \|h_t\|_{\mathcal{L}_t^2} + 1$. This completes the proof of Lemma 13. \square

Using the same approach as that in proving Proposition 5, we can derive the following proposition.

PROPOSITION 6. *Let $0 \leq \delta \leq 1$ with δ satisfying (58). Under Assumptions 1-4 with $\frac{1}{2} \leq r \leq 1$ and $0 < s \leq 1$, if $\lambda_t = |D|^{-\frac{1}{2r+s}}$ for $t = 1, \dots, T$, $|D_1| = \dots = |D_m|$, and m satisfies (22), then with confidence $1 - \delta$, it holds that*

$$\|\bar{Q}_{D,\lambda_t,t}\|_{\mathcal{L}_t^\infty} \leq 2\hat{C}^T (2\mu^{1/2})^{T-t} M \prod_{\ell=t}^{T-1} \left((T - \ell + 2) (2\mu^{1/2})^{\ell-t} + 1 \right) - M, \quad t = 1, \dots, T.$$

D.6. Deriving generalization errors

In this subsection, we derive the generalization error of KRR-DTR and DKRR-DTR. To prove our main theorems, we need the following lemma, which is standard in statistical learning theory.

LEMMA 14. *Let $0 < \delta < 1$, and $\xi \in \mathbb{R}_+$ be a random variable. If $\xi \leq u \log^b \frac{c}{\delta}$ holds with confidence $1 - \delta$ for some $u, b, c > 0$, then $E[\xi] \leq c\Gamma(b+1)u$, where $\Gamma(\cdot)$ is the Gamma function.*

Proof. Since $\xi \leq u \log^b \frac{c}{\delta}$ holds with confidence $1 - \delta$, we have $P[\xi > t] \leq c \exp\{-u^{-1/b}t^{1/b}\}$. Using the probability to expectation formula

$$E[\xi] = \int_0^\infty P[\xi > \varepsilon] d\varepsilon \tag{67}$$

to the positive random variable ξ , we have $E[\xi] \leq c \int_0^\infty \exp\{-u^{-1/b} \varepsilon^{1/b}\} d\varepsilon \leq cu\Gamma(b+1)$. This completes the proof of Lemma 14. \square

With the above foundations, we are in a position to prove our main theorems.

Proof of Theorem 1. It follows from Proposition 2 that

$$\begin{aligned} E \left[\| (Q_{D,\lambda_t,t} - Q_t^*) \|_{\mathcal{L}_t^2} \right] &\leq E \left[\| (L_{K,t} + \lambda_t I)^{1/2} (Q_{D,\lambda_t,t} - Q_t^*) \|_{K,t} \right] \\ &\leq \sum_{\ell=t}^T \mu^{\frac{\ell-t}{2}} E \left[\mathcal{A}_{D,\lambda_\ell,\ell}^{\ell-t+1} \left(\lambda_\ell^r \| h_\ell \|_{\mathcal{L}_\ell^2} + \mathcal{P}_{D,\lambda_\ell,\ell} + \mathcal{S}_{D,\lambda_\ell,\ell} + \mathcal{U}_{D,\lambda_\ell,\ell, Q_\ell^* - Q_{D,\lambda_\ell,\ell}^*} \right) \right]. \end{aligned}$$

For $\lambda_1 = \dots = \lambda_T = |D|^{-\frac{1}{2r+s}}$, it follows from (54), (55), (56), (57), and Proposition 5 that, with confidence $1 - \delta$ with δ satisfying (50), it holds that

$$\begin{aligned} &\mathcal{A}_{D,\lambda_\ell,\ell}^{\ell-t+1} \left(\lambda_\ell^r \| h_\ell \|_{\mathcal{L}_\ell^2} + \mathcal{P}_{D,\lambda_\ell,\ell} + \mathcal{S}_{D,\lambda_\ell,\ell} + \mathcal{U}_{D,\lambda_\ell,\ell, Q_\ell^* - Q_{D,\lambda_\ell,\ell}^*} \right) \\ &\leq 2^{\ell-t} \tilde{C}_1 \bar{C}^T (2\mu^{1/2})^{T-\ell} M \prod_{k=\ell}^{T-1} \left((T-k+2) (2\mu^{1/2})^{k-\ell} + 1 \right) |D|^{\frac{-r}{2r+s}} \log \frac{8T}{\delta}, \end{aligned}$$

where $\tilde{C}_1 := 4 \max_{t=1,\dots,T} \| h_t \|_{\mathcal{L}_t^2} + 16M(\sqrt{C_0} + 1) + 2(\kappa + 1)(\sqrt{C_0} + 1) + 4(\sqrt{C_0} + 1)$. Then it follows from Lemma 14, (50), and (67) that

$$\begin{aligned} E \left[\| Q_{D,\lambda_t,t} - Q_t^* \|_{\mathcal{L}_t^2} \right] &\leq \int_0^\infty P \left[\| Q_{D,\lambda_t,t} - Q_t^* \|_{\mathcal{L}_t^2} > \varepsilon \right] d\varepsilon \\ &\leq \int_0^{8T \exp \left\{ -\frac{2r+s}{4sC_1^*(\log(C_0+1)+2)} |D|^{\frac{2r+s-1}{8r+4s}} \log^{-1} |D| \right\}} d\varepsilon \\ &\quad + \int_{8T \exp \left\{ -\frac{2r+s}{4sC_1^*(\log(C_0+1)+2)} |D|^{\frac{2r+s-1}{8r+4s}} \log^{-1} |D| \right\}}^\infty P \left[\| Q_{D,\lambda_t,t} - Q_t^* \|_{\mathcal{L}_t^2} > \varepsilon \right] d\varepsilon \\ &\leq \tilde{C}_2 T \sum_{\ell=t}^T \mu^{\frac{\ell-t}{2}} 2^{\ell-t} \bar{C}^T (2\mu^{1/2})^{T-\ell} \prod_{k=\ell}^{T-1} \left((T-k+2) (2\mu^{1/2})^{k-\ell} + 1 \right) |D|^{\frac{-r}{2r+s}}, \end{aligned}$$

where \tilde{C}_2 is a constant depending only on \tilde{C}_1 , M , r , s , and C_0 . Noting further (18), we then have

$$\begin{aligned} &E \left[V_1^*(S_1) - V_{\pi_{D,\tilde{\lambda}},1}(S_1) \right] \\ &\leq C_1 \sum_{t=1}^T \mu^{t/2} T \sum_{\ell=t}^T \mu^{\frac{\ell-t}{2}} 2^{\ell-t} \bar{C}^T (2\mu^{1/2})^{T-\ell} \prod_{k=\ell}^{T-1} \left((T-k+2) (2\mu^{1/2})^{k-\ell} + 1 \right) |D|^{\frac{-r}{2r+s}} \end{aligned}$$

for $C_1 = 2\tilde{C}$. This completes the proof of Theorem 1. \square

Proof of Theorem 2. It follows from Proposition 4 that

$$\begin{aligned} E \left[\| \bar{Q}_{D,\lambda_t,t} - Q_t^* \|_{\mathcal{L}_t^2} \right] &\leq E \left[\| (L_{K,t} + \lambda_t I)^{1/2} (\bar{Q}_{D,\lambda_t,t} - Q_t^*) \|_{K,t} \right] \\ &\leq \sum_{\ell=t}^T \prod_{k=t+1}^{\ell} \left(\left(\sum_{j=1}^m \frac{|D_j|}{|D|} \mathcal{W}_{D_j,\lambda_k,k} \mathcal{A}_{D_j,\lambda_k,k} + \mathcal{A}_{D,\lambda_k,k} \right) \mu^{1/2} \right) \end{aligned}$$

$$\begin{aligned}
& \times \left(\sum_{j=1}^m \frac{|D_j|}{|D|} \mathcal{W}_{D_j, \lambda_\ell, \ell} \mathcal{A}_{D_j, \lambda_\ell, \ell} \left(\lambda_\ell^r \|h_\ell\|_{\mathcal{L}_\ell^2} + \mathcal{P}_{D_j, \lambda_\ell, \ell} + \bar{\mathcal{S}}_{D_j, \lambda_\ell, \ell} + \mathcal{U}_{D_j, \lambda_\ell, \ell, Q_\ell^* - \bar{Q}_{D_j, \lambda_\ell, \ell}^*} \right) \right. \\
& \left. + \mathcal{A}_{D, \lambda_\ell, \ell} \left(\lambda_\ell^r \|h_\ell\|_{\mathcal{L}_\ell^2} + \mathcal{P}_{D, \lambda_\ell, \ell} + \bar{\mathcal{S}}_{D, \lambda_\ell, \ell} + \mathcal{U}_{D, \lambda_\ell, \ell, Q_\ell^* - \bar{Q}_{D, \lambda_\ell, \ell}^*} \right) + \mathcal{U}_{D, \lambda_\ell, \ell, Q_\ell^*} \right].
\end{aligned}$$

But (22), (54), (58), (63), (64), (65), (66), and Proposition 6 yield that for any $t = 1, \dots, T$, with confidence

$1 - \delta/2$, it holds that $\left(\sum_{j=1}^m \frac{|D_j|}{|D|} \mathcal{W}_{D_j, \lambda_t, t} \mathcal{A}_{D_j, \lambda_t, t} + \mathcal{A}_{D, \lambda_t, t} \right) \leq 2$ and

$$\begin{aligned}
& \sum_{j=1}^m \frac{|D_j|}{|D|} \mathcal{W}_{D_j, \lambda_\ell, \ell} \mathcal{A}_{D_j, \lambda_\ell, \ell} \left(\lambda_\ell^r \|h_\ell\|_{\mathcal{L}_\ell^2} + \mathcal{P}_{D_j, \lambda_\ell, \ell} + \bar{\mathcal{S}}_{D_j, \lambda_\ell, \ell} + \mathcal{U}_{D_j, \lambda_\ell, \ell, Q_\ell^* - \bar{Q}_{D_j, \lambda_\ell, \ell}^*} \right) \\
& \leq \tilde{C}_3 m |D|^{\frac{1-2r-s}{4r+2s}} \log |D| |D|^{-\frac{r}{2r+s}} \hat{C}^T (2\mu^{1/2})^{T-t} \prod_{\ell=t}^{T-1} \left((T-\ell+2) (2\mu^{1/2})^{\ell-t} + 1 \right) \log \frac{40mT}{\delta} \\
& \leq \tilde{C}_3 |D|^{-\frac{r}{2r+s}} \hat{C}^T (2\mu^{1/2})^{T-t} \prod_{\ell=t}^{T-1} \left((T-\ell+2) (2\mu^{1/2})^{\ell-t} + 1 \right) \log \frac{40}{\delta},
\end{aligned}$$

where we use $\log ab \leq (\log a + 1) \log b$ for $a, b \geq 3$ in the last inequality, and

$$\tilde{C}_3 := 6MC_1^* \frac{2s}{2r+s} (\log(C_0 + 1) + 2) \left(\max_{t=1, \dots, T} \|h_t\|_{\mathcal{L}_t^2} + 8(\sqrt{C_0} + 1) \right) + 2(\kappa + 1)(\sqrt{C_0} + 1).$$

Similarly, we can derive that with confidence $1 - \delta/2$, it holds that

$$\begin{aligned}
& \mathcal{A}_{D, \lambda_\ell, \ell} \left(\lambda_\ell^r \|h_\ell\|_{\mathcal{L}_\ell^2} + \mathcal{P}_{D, \lambda_\ell, \ell} + \bar{\mathcal{S}}_{D, \lambda_\ell, \ell} + \mathcal{U}_{D, \lambda_\ell, \ell, Q_\ell^* - \bar{Q}_{D, \lambda_\ell, \ell}^*} \right) + \mathcal{U}_{D, \lambda_\ell, \ell, Q_\ell^*} \\
& \leq \tilde{C}_4 |D|^{-\frac{r}{2r+s}} \hat{C}^T (2\mu^{1/2})^{T-t} \prod_{\ell=t}^{T-1} \left((T-\ell+2) (2\mu^{1/2})^{\ell-t} + 1 \right) \log \frac{40T}{\delta},
\end{aligned}$$

where $\tilde{C}_4 := 6M \left(\max_{t=1, \dots, T} \|h_t\|_{\mathcal{L}_t^2} + 8(\sqrt{C_0} + 1) \right) + 2(\kappa + 1)(\sqrt{C_0} + 1)$. Hence, we have from Lemma 14 that

$$\begin{aligned}
E \left[\left\| \bar{Q}_{D, \lambda_t, t} - Q_t^* \right\|_{\mathcal{L}_t^2} \right] & \leq 40Tm \exp \left\{ - \frac{2r+s}{4sC_1^*(\log(C_0 + 1) + 2)} |D|^{\frac{2r+s-1}{16r+8s}} m^{-1/2} \log^{-1} |D| \right\} \\
& + 80(\tilde{C}_3 + \tilde{C}_4)T |D|^{-\frac{r}{2r+s}} \hat{C}^T (2\mu^{1/2})^{T-t} \prod_{\ell=t}^{T-1} \left((T-\ell+2) (2\mu^{1/2})^{\ell-t} + 1 \right) \\
& \leq C_2 T |D|^{-\frac{r}{2r+s}} \hat{C}^T (2\mu^{1/2})^{T-t} \prod_{\ell=t}^{T-1} \left((T-\ell+2) (2\mu^{1/2})^{\ell-t} + 1 \right),
\end{aligned}$$

where C_2 is a constant depending only on $\max_{t=1, \dots, T} \|h_t\|_{\mathcal{L}_t^2}$, C_0 , κ , M , r , and s . This together with (18) completes the proof of Theorem 2. \square

References

Almirall D, Chronis-Tuscano A (2016) Adaptive interventions in child and adolescent mental health. *Journal of Clinical Child and Adolescent Psychology* 45(4):383–395.

Blanchard G, Krämer N (2016) Convergence rates of kernel conjugate gradient for random design regression. *Analysis and Applications* 14(06):763–794.

Caponnetto A, De Vito E (2007) Optimal rates for the regularized least-squares algorithm. *Foundations of Computational Mathematics* 7(3):331–368.

Chakraborty B, Moodie EEM (2013) *Statistical Reinforcement Learning* (New York: Springer).

Duan Y, Jin C, Li Z (2021) Risk bounds and rademacher complexity in batch reinforcement learning. Meila M, Zhang T, eds., *Proceedings of the 38th International Conference on Machine Learning*, volume 139 of *Proceedings of Machine Learning Research*, 2892–2902 (PMLR).

Even-Dar E, Mansour Y (2003) Learning rates for q-learning. *Journal of Machine Learning Research* 5:1–25.

Fan J, Yang Z, Xie Y, Wang Z (2020) A theoretical analysis of deep q-learning. *arXiv preprint arXiv:1901.00137v3* .

Figueiredo Prudencio R, Maximo MROA, Colombini EL (2024) A survey on offline reinforcement learning: Taxonomy, review, and open problems. *IEEE Transactions on Neural Networks and Learning Systems* 35(8):10237–10257.

François-Lavet V, Henderson P, Islam R, Bellemare MG, Pineau J (2018) An introduction to deep reinforcement learning. *Foundations and Trends in Machine Learning* 11(3-4):219–354.

Fujimoto S, van Hoof H, Meger D (2018) Addressing function approximation error in actor-critic methods. Dy J, Krause A, eds., *Proceedings of the 35th International Conference on Machine Learning*, volume 80 of *Proceedings of Machine Learning Research*, 1587–1596 (PMLR).

Glorot X, Bengio Y (2010) Understanding the difficulty of training deep feedforward neural networks. *Proceedings of the 13th International Conference on Artificial Intelligence and Statistics*, 249–356 (Sardinia, Italy).

Goldberg Y, Kosorok MR (2012) Q-learning with censored data. *Annals of Statistics* 40(1):529–560.

Goodfellow I, Bengio Y, Courville A (2016) *Deep Learning* (MIT Press).

Gosavi A (2009) Reinforcement learning: A tutorial survey and recent advances. *INFORMS Journal on Computing* 21(2):178–192.

Guo ZC, Lin SB, Zhou DX (2017) Learning theory of distributed spectral algorithms. *Inverse Problems* 33(7):074009.

Györfi L, Kohler M, Krzyzak A, Walk H (2006) *A Distribution-Free Theory of Nonparametric Regression* (Springer Science & Business Media).

Haarnoja T, Zhou A, Hartikainen K, Tucker G, Ha S, Tan J, Kumar V, Zhu H, Gupta A, Abbeel P, Levine S (2019) Soft actor-critic algorithms and applications. *arXiv preprint arXiv:1812.05905*.

He K, Zhang X, Ren S, Sun J (2015) Delving deep into rectifiers: surpassing human-level performance on imagenet classification. *Proceedings of the 2015 IEEE International Conference on Computer Vision (ICCV)*, 1026–1034, ICCV '15 (USA: IEEE Computer Society).

Humphrey K (2017) *Using reinforcement learning to personalize dosing strategies in a simulated cancer trial with high dimensional data*. Master's thesis, The University of Arizona, Tucson, URL <http://hdl.handle.net/10150/625341>.

Ishigooka J, Murasaki M, Miura S, Group TOLPIS (2000) Olanzapine optimal dose: Results of an open-label multicenter study in schizophrenic patients. *Psychiatry and Clinical Neurosciences* 54(4):467–478.

Janner M, Fu J, Zhang M, Levine S (2019) When to trust your model: model-based policy optimization. *Proceedings of the 33rd International Conference on Neural Information Processing Systems*, 12519–12530 (Red Hook, NY, USA: Curran Associates Inc.).

Kearns MJ, Singh SP (1998) Finite-sample convergence rates for q-learning and indirect algorithms. *Proceedings of the 11th International Conference on Neural Information Processing Systems*, 996–1002, NIPS'98 (Cambridge, MA, USA: MIT Press).

Levine S, Kumar A, Tucker G, Fu J (2020) Offline reinforcement learning: Tutorial, review, and perspectives on open problems. *arXiv preprint arXiv:2005.01643*.

Lillicrap TP, Hunt JJ, Pritzel A, Heess N, Erez T, Tassa Y, Silver D, Wierstra D (2016) Continuous control with deep reinforcement learning. Bengio Y, LeCun Y, eds., *Proceedings of the 4th International Conference on Learning Representations* (San Juan, Puerto Rico).

Lin SB, Guo X, Zhou DX (2017) Distributed learning with regularized least squares. *Journal of Machine Learning Research* 18(92):1–31.

Lin SB, Wang D, Zhou DX (2020) Distributed kernel ridge regression with communications. *Journal of Machine Learning Research* 21(93):1–38.

Lin SB, Zhou DX (2018) Distributed kernel-based gradient descent algorithms. *Constructive Approximation* 47(2):249–276.

Liu S, Su H (2022) Provably efficient kernelized q-learning. *arXiv preprint arXiv:2204.10349* .

Meister M, Steinwart I (2016) Optimal learning rates for localized svms. *Journal of Machine Learning Research* 17(194):1–44.

Mnih V, Badia AP, Mirza M, Graves A, Lillicrap T, Harley T, Silver D, Kavukcuoglu K (2016) Asynchronous methods for deep reinforcement learning. Balcan MF, Weinberger KQ, eds., *Proceedings of the 33rd International Conference on Machine Learning*, volume 48 of *Proceedings of Machine Learning Research*, 1928–1937 (New York, New York, USA: PMLR).

Murphy SA (2005a) An experimental design for the development of adaptive treatment strategies. *Statistics in Medicine* 24(10):1455–1481.

Murphy SA (2005b) A generalization error for q-learning. *Journal of Machine Learning Research* 6(37):1073–1097.

Oh EJ, Qian M, Cheung YK (2022) Generalization error bounds of dynamic treatment regimes in penalized regression-based learning. *Annals of Statistics* 50(4):2047–2071.

Ong HY, Chavez K, Hong A (2015) Distributed deep q-learning. *arXiv preprint arXiv:1508.04186* .

Oroojlooyjadid A, Nazari M, Snyder LV, Takáč M (2022) A deep q-network for the beer game: Deep reinforcement learning for inventory optimization. *Manufacturing and Service Operations Management* 24(1):285–304.

Padmanabhan R, Meskin N, Haddad WM (2017) Reinforcement learning-based control of drug dosing for cancer chemotherapy treatment. *Mathematical Biosciences* 293:11–20.

Pinelis I (1994) Optimum bounds for the distributions of martingales in banach spaces. *Annals of Probability* 22(4):1679–1706.

Raghu A, Komorowski M, Celi LA, Szolovits P, Ghassemi M (2017) Continuous state-space models for optimal sepsis treatment: A deep reinforcement learning approach. Doshi-Velez F, Fackler J, Kale D, Ranganath R, Wallace B, Wiens J, eds., *Machine Learning for Healthcare Conference*, volume 68 of *Proceedings of Machine Learning Research*, 147–163 (PMLR).

Rudi A, Camoriano R, Rosasco L (2015) Less is more: Nyström computational regularization. *Proceedings of the 28th International Conference on Neural Information Processing Systems*, volume 1 of *NIPS'15*, 1657–1665 (Cambridge, MA, USA: MIT Press).

Schulman J, Wolski F, Dhariwal P, Radford A, Klimov O (2017) Proximal policy optimization algorithms. *arXiv preprint arXiv: 1707.06347*.

Smale S, Zhou DX (2005) Shannon sampling II: Connections to learning theory. *Applied and Computational Harmonic Analysis* 19(3):285–302.

Socinski MA, Stinchcombe TE (2007) Duration of first-line chemotherapy in advanced non small-cell lung cancer: less is more in the era of effective subsequent therapies. *Journal of Clinical Oncology* 25(33):5155–5157.

Sutton RS, Barto AG (2018) *Reinforcement Learning: An Introduction* (MIT press).

Sutton RS, McAllester D, Singh S, Mansour Y (1999) Policy gradient methods for reinforcement learning with function approximation. *Proceedings of the 12th International Conference on Neural Information Processing Systems*, 1057–1063, NIPS'99 (Cambridge, MA, USA: MIT Press).

Tseng HH, Luo Y, Cui S, Chien JT, Ten Haken RK, Naqa IE (2017) Deep reinforcement learning for automated radiation adaptation in lung cancer. *Medical Physics* 44(12):6690–6705.

Tsiatis AA, Davidian M, Holloway ST, Laber EB (2019) *Dynamic Treatment Regimes: Statistical Methods for Precision Medicine* (Chapman and Hall/CRC).

Wainwright MJ (2019) Variance-reduced q-learning is minimax optimal. *arXiv preprint arXiv:1906.04697*.

Wang R, Foster DP, Kakade SM (2020) What are the statistical limits of offline RL with linear function approximation? *arXiv preprint arXiv:2010.11895*.

Watkins CJ, Dayan P (1992) Q-learning. *Machine Learning* 8(3-4):279–292.

Xu X, Hu D, Lu X (2007) Kernel-based least squares policy iteration for reinforcement learning. *IEEE Transactions on Neural Networks* 18(4):973–992.

Yu C, Liu J, Nemati S, Yin G (2021) Reinforcement learning in healthcare: A survey. *ACM Computing Surveys* 55(1):1–36.

Zhang Y, Duchi J, Wainwright M (2015) Divide and conquer kernel ridge regression: A distributed algorithm with minimax optimal rates. *Journal of Machine Learning Research* 16(102):3299–3340.

Zhao Y, Kosorok MR, Zeng D (2009) Reinforcement learning design for cancer clinical trials. *Statistics in Medicine* 28(26):3294–3315.